Technical report
TR - 173

Ministerie van Verkeer en Waterstaat
Koninklijk Nederlands
Meteorologisch Instituut

Measurements of the structure parameter of vertical wind-velocity in the atmospheric boundary layer

R. van der Ploeg

De Bilt, 1995

Technical report; TR - 173

De Bilt 1995

Postbus 201
3730 AE De Bilt
Wilhelminalaan 10
Telefoon 030-206 911
Telefax 030-210 407

Afstudeerverslag TU Delft

UDC: 551.501.755
551.510.522
551.558

ISSN: 0169-1708

ISBN: 90-369-2072-8

Measurements of the structure parameter of vertical wind-velocity in the atmospheric boundary layer

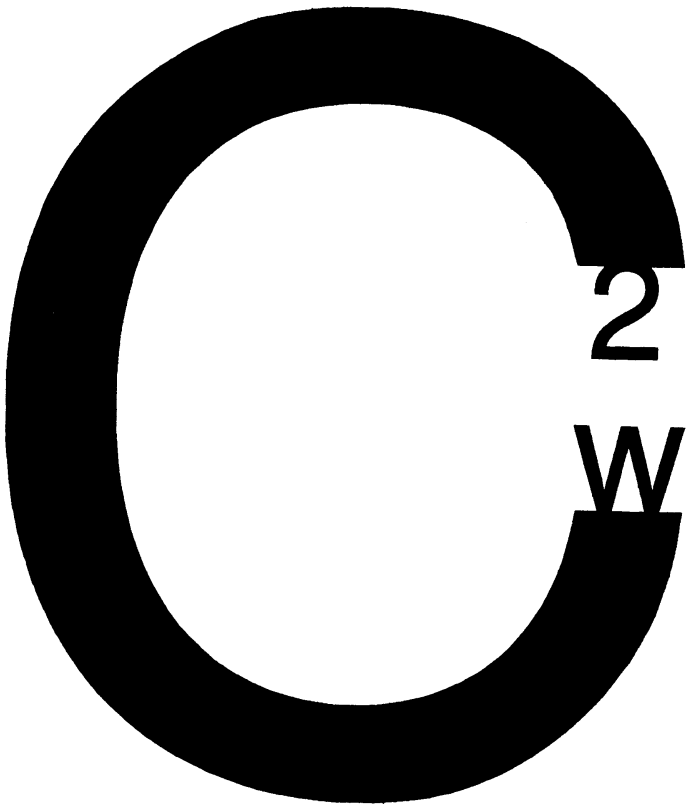

Afstudeerverslag

aan de TU-Delft,

faculteit der Technische Natuurkunde,

sectie Warmtetransport

Rik van der Ploeg

december 1991

CONTENTS

		page
	Samenvatting, Abstract	
1	Introduction	1
2	**Theoretical relations of the structure parameter of vertical velocity**	3
2.1	The structure parameter in the inertial subrange	3
2.2	The original similarity theory	6
2.3	The modified similarity theory	7
2.4	Scaling relations	9
3	**Correction of the structure parameter of vertical wind-velocity measured by a sonic anemometer**	11
3.1	Measurement principle of the sonic anemometer	12
3.2	Signal-handling of the SONIC DAT-300	14
3.3	Calculation of the correction factors	17
3.3.1	Evaluation of the response term	20
3.3.2	Influence of line-averaging	22
4	**Measurements of the structure parameter at three sites**	27
4.1	Crau	27
4.2	Speuld	28
4.3	Cabauw	29
4.4	Data-handling	31

page

5 **Results** 33

5.1 Inertial subrange limits 33

5.2 Correction factors of different response-functions 36

5.3 Correction of the measurements 38

5.4 Scaling relations 40

6 **Discussion, Conclusions** 43

6.1 The limits of the inertial subrange and isotropy 43

6.2 The structure parameter correction 44

6.3 The scaling relations 44

Appendices

A1 Corrections for U and u_* measured by a sonic anemometer 46

A2 Sonic specifications 48

A3 Dataset description files 49

B1 Structure parameter correction programs 59

B2 Programs for Crau 68

B3 Programs for Speuld 72

B4 Programs for Cabauw 74

Literature 81

Samenvatting

De structuurparameter van de verticale windsnelheid bevat informatie over de kleine schalen van het turbulente windveld. Onder de aanname van de aanwezigheid van een inertial subrange kan ook de turbulente energie-dissipatiesnelheid afgeleid worden. In deze studie wordt de signaalverwerking van een Kaijo Denki DAT-300 sonische anemometer geanalyseerd. Op basis van deze analyse worden correctieprocedures ontwikkeld voor temporele en ruimtelijke responsverliezen. In deze correctieprocedures wordt aan genomen dat de turbulentie een inertial subrange bevat en dat in deze range de turbulentie isotroop is. Drie experimentele datasets worden gebruikt, een grasland locatie (Cabauw), een locatie met droog oppervlak en stenen (Crau) en een bos locatie (Garderen). Door het vergelijken van structuurparameters gebaseerd op verschillende tijdsintervallen konden de correctieprocedures getest worden. Goede resultaten werden bereikt ondanks enige onzekerheid over de filterkarakteristieken van de sonische anemometer elektronica. De aannames over de inertial-subrange en isotropie werden vervolgens onderzocht aan de hand van de verhoudingen van structuurparameters voor verschillende tijdsintervallen. Deze test leverde criteria op voor de verhouding tussen de meethoogte (z) en de grootte van de eddie waarnaar we kijken (D). Voor stabiele omstandigheden: $z/D>6$. Voor onstabiel omstandigheden: $z/D>3$. Deze criteria zijn vergelijkbaar met de criteria die Kaimal et al. (1972) vonden voor isotropie en inertial-subrange. Kort is aandacht besteed aan de schalingsrelaties voor de structuurparameter van de verticale wind. De resultaten blijken goed overeen te komen met wat verwacht mag worden op grond van schalingsrelaties voor dissipatie. De structuurparameter van de verticale wind blijkt na correctie goed bruikbaar voor verdere analyse.

Abstract

The structure parameter of the vertical wind gives information about the small scales of the turbulent windfield. In particular it gives an estimate of the energy dissipation rate if the presence of an inertial subrange can be assumed. In this study the signal processing chain of a Kaijo Denki DAT-300 sonic anemometer is analyzed. From this analysis procedures are obtained to correct measured structure parameters for temporal and spatial losses. In these correction procedures it is assumed that the turbulence has an inertial subrange and is isotropic in this range. Three surface layer datasets are used, one grassland site (Cabauw), one dry stony surface site (Crau) and one forest site (Garderen). By comparing measured structure parameters at different time intervals the correction procedures could be tested. Despite some uncertainties concerning the filter characteristics of the sonic anemometer electronics, the correction procedure gives good results. To verify the assumptions about the inertial subrange and isotropy, a test based on the ratios of structure parameters with different lag times was used. The test produced criteria for the ratio of the measurement height (z) and the eddy-size (D). In the stable case: $z/D>6$. in the unstable case: $z/D>3$. These criteria are comparable with the criteria obtained by Kaimal et al. (1972) for isotropy in the inertial subrange. It is found that structure parameters derived from lag times less then the cycle time of the sonic anemometer (53 msec) can not be corrected. Short attention is paid to scaling relations of the structure parameter of vertical wind. The results are consistent with dissipation scaling relations found in the literature. After correction the structure parameter of the vertical wind appears to be a tractable quantity for further analysis.

1 Introduction

Information about the small scale structure of the turbulence is important for a number of reasons. Structure parameters of temperature and humidity are relevant in the study of electro-magnetic wave propagation and acoustic wave propagation through the atmosphere. Structure parameters of the wind components give information about the energy flow through the turbulent cascade from large scale energy containing eddies to small scale dissipative eddies. The scaling behaviour of the structure parameter of the wind gives information about the length scale of the energy containing eddies. This opens the possibility to derive an estimate of the zero-plane over ill defined surfaces like forests when the scaling relation for low-vegetation are established. New tools in atmospheric research like wind profiler and doppler sodar make use of the atmospheric characteristics described by structure parameters. Finally structure parameters can be used to estimate turbulent fluxes of heat, moisture and momentum through empirical determined similarity functions.

The measurement of structure parameters in the atmospheric surface layer poses serious demands on the spectral response characteristics of the instrument. Cold wire and Ly-α hygrometer were used by Kohsiek (1982) to obtain structure parameters of temperature and humidity. For wind components hot-wires are suitable but difficult to operate outside the laboratory. Another way to proceed is to use more robust instruments with large but known spectral characteristics and to correct the data for these losses. To calculate spectral losses one has to make assumptions about the spectrum of the turbulence. One therefor has to be careful to draw to detailed conclusions on the basis of such corrected measurements.

Here we concentrate on the estimation of the structure parameter of the vertical wind from measurements with a Kaijo Denki DAT-300 sonic anemometer. The relevant corrections due to temporal and spatial averaging in the instrument are obtained. A number of software routines are described which enable to perform the corrections on the measurements. Field data of CRAU (Kohsiek et al., 1987), Cabauw (Bouwman, 1990) and Speulderbos (Bosveld et al., 1995) are used to test the applicability of the correction

procedures. The data are analyzed on the basis of Monin-Obhukov similarity theory.

2 THEORETICAL RELATIONS OF THE STRUCTURE PARAMETER OF VERTICAL WIND-VELOCITY

2.1 The Structure parameter in the inertial subrange

Before we discuss the behaviour of the second-order structure function parameter of vertical velocity in the inertial subrange, and its relation to other quantities, we will look first at structure functions in general. The nth-order structure function of quantity χ is defined by

$$D_\chi^n(\Delta x) = \langle (\chi - \chi')^n \rangle \tag{2.1}$$

Here Δx is the distance that separates the two points at which χ and χ' are measured. The brackets enclosing the right-hand part of this expression indicate that the equation in between has to be time-averaged. It is striking that the widely used 2nd-order structure function is called "the" structure function by many authors. They do not refer to a general system of structure functions, with the second-order function as a particular case. This habit ignores the importance of the higher-order structure functions which are usually more sensitive to theoretical refinements, as stated e.g. by Van Atta and Chen (1970).

Anyhow, many measurements have been made in order to study the behaviour of the second-order structure functions and their related structure function parameters in the inertial subrange. Mostly the structure parameters of temperature, humidity, temperature-humidity, refractive index and velocity are involved in these studies.
This study focuses on the second order structure function parameter of vertical wind velocity, shortly called: "the" structure parameter of vertical velocity. This parameter can be obtained from $D_w^2(\Delta x)$ by

$$C_w^2 = \frac{\left\langle \left\{ w(\vec{x}) - w(\vec{x}+\overrightarrow{\Delta x}) \right\}^2 \right\rangle}{\Delta x^{2/3}} \tag{2.2}$$

Here $\vec{x}$ and $\vec{x}+\overrightarrow{\Delta x}$ denote the points in space where w, the vertical wind-velocity, is measured. This structure parameter is defined with respect to the space-interval $\overrightarrow{\Delta x}$. This interval can be related to a time-interval, using Taylors hypothesis

$$\vec{x} = \vec{U}t \tag{2.3}$$

in which $\vec{U}$ is the vector of horizontal wind-velocity. We choose a frame of reference with the x-axis in the direction of the mean wind. The reliability of using the Taylor hypothesis for structure parameters was checked by Kohsiek (1982). Using (2.3) we also write for C_w^2

$$C_w^2 = \frac{\left\langle \{ w(t) - w(t+\Delta t) \}^2 \right\rangle}{(U\Delta t)^{2/3}} \tag{2.4}$$

Δt is the time-interval over which the structure parameter is measured. A question can arise according to the 2/3-exponent in the denominator of the C_w^2 definition. This exponent is chosen on ground of the relations in the inertial subrange, mentioned below. The denominator is such that the structure parameter in the inertial subrange remains independent of the space or time interval. We talk about the inertial subrange, but there are more ranges in turbulence. These ranges consist of eddies of different sizes. The "outer" range, containing the big eddies, depends on the geometry of the flow. In the turbulent air-flow of the atmospheric boundary layer these eddies have sizes in the order of the measurement height. On the other end their is an "inner" range, holding the very small eddies. At this small scale, viscous dissipation plays the important role. Here kinetic energy is destroyed and heat is created. Between the "outer" and the "inner" range a non-lineair mechanism acts, vortex stretching, creating smaller eddies from larger eddies (Tennekes & Lumley, 1972).

Of special interest is the inertial subrange. This range consist of eddies that are much smaller than the measurement height, but much larger than the small scale. In the inertial subrange the turbulence starts to become isotropic. Since isotropy only appears at small scales, it is called local isotropy. The energy spectrum of the inertial subrange takes a special form, the so called 5/3-law. This is caused by the separation of the small and the big scales at high Reynolds numbers. At small scales velocity components are isotropic. At long wave end the different components of the energy spectrum exchange still energy in order to become isotropic. Therefore not the whole inertial subrange is isotropic. The limits of isotropy can be verified by investigation of the separate components in the flow. When a single component of the wind exhibits inertial subrange behaviour, energy exchange takes place no longer, so the flow is isotropic.

One of the conditions to be satisfied for isotropic inertial subrange behaviour is: $S_w(k)/S_u(k) = 4/3$. Here S_u is the spectrum of the longitudinal component of wind-velocity, k is the wavenumber. From the ratio S_w/S_u the relation between the Kolmogorov constant of vertical velocity, α_w, and the Kolmogorov constant of longitudinal velocity, α_u, is known: $\alpha_w = 4/3\alpha_u$. Kaimal et al. (1972) used the 4/3-condition to test for isotropy. They split their results in several stability classes, see figure 5.1. Isotropy is important, because for the derivation of specific scaling relations for the structure parameters, and also for the derivation of the structure parameter correction, our measurements must be within the isotropic part of the inertial subrange. Next to the 4/3-condition, Van Atta and Chen (1970) found for the behaviour of the structure functions (and of their parameters), that deviations from inertial subrange form are good indicators of the subrange limits.

We use the ratios of two structure parameters of the vertical component of wind-velocity, measured with respect to different space-intervals, to test for subrange behaviour. The intervals must differ a lot, e.g. a factor two. The denominator in the ratio is the C_w^2 with the biggest interval. If the upper structure parameter in the ratio is in the inertial subrange, and the lower not anymore, the ratio of the two will increase. This will happen if the biggest space interval, used to obtain a structure parameter, is no longer

much smaller than the measurement height. In this way we test for inertial subrange behaviour in a single velocity component, as explained this might be a representative test for isotropy.

2.2 The original similarity theory

According to the original version of Kolmogorov's similarity theory (see Hinze, 1957) the velocity structure functions in the inertial subrange depend only on Δx and the dissipation ε

$$\langle (w-w')^n \rangle = C_n (\varepsilon \Delta x)^{n/3} \tag{2.5}$$

in which C_n are universal constants, n is an integer value greater than zero. This shows that the structure parameter can be used for experimental determination of ε:

$$C_w^2 = C_2 \varepsilon^{2/3} \tag{2.6}$$

The constant C_2 can be calculated from other relationships in the inertial subrange. One of these is the relation between C_w^2 and the inertial subrange spectrum of vertical velocity S_w. By Fourier transformation of the correlation function we obtain

$$S_w(k) = 0.25 C_w^2 k^{-5/3} \tag{2.7}$$

in which 0.25 is a mathematical constant (Wyngaard et al.,1971). The spectrum of vertical velocity can also be described by the inertial subrange relation

$$S_w(k) = \alpha_w \varepsilon^{2/3} k^{-5/3} \tag{2.8}$$

Using these two equations, we can determine the constant C_2

$$C_2 = 4\alpha_w \tag{2.9}$$

As mentioned before, these specific relations between C_w^2, $S_w(k)$ and ε are only valid in the inertial subrange. We can use the 4/3 ratio between α_w and α_u to determine C_2 if α_w is not known.

2.3 The modified similarity theory

In 1962 Kolmogorov and Obukhov introduced some modifications to the original similarity theory. A third hypothesis was formulated by Kolmogorov (1962), suggesting that the intermittency of the dissipation rate might be represented by a lognormal probability distribution, which affects the spectra and structure functions in the inertial subrange. The dissipation ε is an intermittent variable because its variance is large compared to the square of its mean value. This model is called the lognormal (LN) model.

Later on other models have been developed, like for example the β-model of Frisch, Sulem & Nelkin (1978). The latter is based on a fractal model of ε, in which the flux of energy is transferred to a fixed fraction of the eddies. Anselmet et al.(1984) compared the LN and the β-model. We consider the effects of the different models on the derived C_w^2-equations. All models lead to the following equation for the second order structure function in the inertial subrange

$$D_w^2(\Delta x) = C_2^* \varepsilon^{2/3} \Delta x^{2/3} \left(\frac{l}{\Delta x}\right)^{\mu_{2/3}} \tag{2.10}$$

$\mu_{2/3}$ is the deviation of the exponent from the 2/3-law. C_2^* is not an absolute constant, but may depend on the macrostructure of the flow (Van Atta and Chen, 1970); l is the length scale of the energy containing eddies. We deduce from (2.10) that the structure in the inertial subrange no longer just depends on ε and r, but also on l. For the different models, $\mu_{2/3}$ takes different values:

$$\begin{aligned} \text{LN} &: \mu_{2/3} = \frac{1}{9}\mu \\ \beta &: \mu_{2/3} = \frac{1}{3}\mu \end{aligned} \tag{2.11}$$

Here μ is the exponent in the equation which describes the behaviour of the autocorrelation of ε in the inertial subrange (Tennekes, 1973)

$$\left\langle \varepsilon(\vec{x})\, \varepsilon\left(\vec{x} + \overrightarrow{\Delta x}\right) \right\rangle \sim \left(\frac{1}{\Delta x}\right)^{\mu} \tag{2.12}$$

By now C_w^2 and ε appear to have a more complicated relationship

$$C_w^2 = C_2^* \left(\frac{1}{\Delta x}\right)^{\mu_{2/3}} \varepsilon^{2/3} \tag{2.13}$$

We use the results of Anselmet et al. (1984), they obtained $\mu_{2/3} = -0.05$ and $\mu = 0.2$. As we see, this value of $\mu_{2/3}$ lies between the LN and the β-model. The factor $C_2^*(l)^{\mu_{2/3}}$ appears to be a very smooth function of l. This factor has a dimension, so we cannot state that it is equal to the constant C_2 from equation (2.6), as Anselmet et al. did, with use of the Kolmogorov scales. Comparison of (2.6) with (2.13) makes sure that C_2 in fact is a function of $\left(\frac{1}{\Delta x}\right)^{\mu_{2/3}}$. The exponent $\mu_{2/3}$ is so small that C_2 seems to be a constant. From the relation between C_2 and the Kolmogorov constant of vertical velocity, the latter appears to be a smooth function of $l/\Delta x$:

$$\alpha_w = 0.25 C_2^* \left(\frac{1}{\Delta x}\right)^{\mu_{2/3}} \tag{2.14}$$

The modifications made to the original Kolmogorov theory have some consequences for the correction of the structure parameter measurements, due to a change in the description of the inertial subrange. Moreover, if these corrections are carried out and a correct C_w^2 is obtained, the ratios between the structure parameters measured with respect to different time-intervals, $\Delta t_{1,2}$, and thus to different Δx, must follow equation (2.13).

This yields:

$$\frac{C^2_{w_{\Delta t_1}}}{C^2_{w_{\Delta t_2}}} = \left(\frac{\Delta t_2}{\Delta t_1}\right)^{\mu_{2/3}} \tag{2.15}$$

So the ratio of the two structure parameters is not exactly unity, but a few percent lower. If $\Delta t_2 = 2\Delta t_1$, the ratio becomes 0.97, if $\Delta t_2 = 4\Delta t_1$, we obtain 0.93.

2.4 Scaling relations

Expected scaling relations of C_w^2 can be derived using the relation between the dissipation ε and the structure parameter, as given by (2.6) We assume we have a quasi-steady, locally homogeneous surface layer. The structure of such a layer follows Monin-Obukhov similarity, which means that properly nondimensionalized statistic variables of the turbulent flow are universal functions of the stability parameter z/L. Here z is the measurement height and L is the Obukhov length, defined by

$$L = \frac{-u_*^3 T}{\kappa g \overline{w\theta_v}} \tag{2.16}$$

Here u_*, called the friction velocity, is the square root of the absolute kinematic surface stress per unit air density exerted by the wind on the surface, T is the mean temperature, κ is the Von Kármán constant, g is the acceleration of gravity and $\overline{w\theta_v}$ is the turbulent virtual temperature flux. In the surface layer it is convenient to nondimensionalize the velocity structure parameters with the height z and with u_*. The dimensionless structure parameter becomes a function of the stability parameter

$$\frac{C_w^2 z^{2/3}}{u_*^2} = f_w(z/L) \tag{2.17}$$

Using the same scales and Von Kármán's constant, the dimensionless dissipation becomes

$$\varepsilon = \frac{u_*^3}{\kappa z}\phi_\varepsilon(z/L) \tag{2.18}$$

From (2.6) and (2.9) we then obtain:

$$f_w(z/L) = 4\alpha_w \kappa^{-2/3}\{\phi_\varepsilon(z/L)\}^{2/3} \tag{2.19}$$

Thus we can calculate the expected scaling relations of the structure parameters of vertical velocity from the scaling relations of the dimensionless dissipation. Conversely we can calculate $\phi_\varepsilon(z/L)$ from the measured $f_w(z/L)$.

From published equations the most commenly given is the equation estimated by Wyngaard and Coté (1971), using the Kansas-data

$$\begin{aligned} \phi_\varepsilon\left(\frac{z}{L}\right) &= \left(1 + 0.5\left|\frac{z}{L}\right|^{2/3}\right)^{3/2} \qquad (z/L < 0) \\ \phi_\varepsilon\left(\frac{z}{L}\right) &= \left(1 + 2.5\left(\frac{z}{L}\right)^{3/5}\right)^{3/2} \qquad (z/L > 0) \end{aligned} \tag{2.20}$$

Other investigators proposed different equations (see §5.4). We assume α_u to be approximately constant and equal to 0.5, as obtained from Kansas data, thus $\alpha_w = \frac{4}{3}\cdot 0.5$. Taking $\kappa = 0.41$ (Wieringa, 1980) the expected scaling equations for C_w^2 become, using (2.19)

$$f_w(z/L) = 4.8\{\phi_\varepsilon(z/L)\}^{2/3} \tag{2.21}$$

In chapter 5 we will compare these theoretical equations with the measurements of C_w^2.

3 CORRECTION OF THE 2-ND ORDER STRUCTURE FUNCTION MEASURED BY A SONIC ANEMOMETER

Measurements of the structure parameter of vertical wind-speed with a sonic anemometer will not give us the true value of this quantity. We have to correct the measurements before we can use them. This correction is related to several effects. Firstly the measured velocity is not estimated at a single point but averaged over a vertical path, in our case a path of 0.20 metres. This line-averaging effect causes spectral losses of the vertical wind-velocity signal. An equation which describes this can be found in paragraph 3.1

The second effect depends on the sonic anemometer type in use. In this study we use a Kaijo Denko DAT-300 sonic anemometer, which measures vertical velocity by sending a pulsed sound-wave upwards and subsequently downwards, using the same transducers. Obviously there must be a time-interval between the two pulses. Although it is not a large interval, the time-interval causes distortion of the velocity-signal, which is described further in paragraph 3.1

Thirdly the wind-speed signal is distorted even more during its trip through the SONIC signal-handling system. It has to pass several non-ideal systems, depending again on the sonic anemometer type in use, which affect the signal in a way that can be described by their impulse-response functions (Oppenheim et al. 1983). We follow the velocity signal on its way through the SONIC in paragraph 3.2.

The vertical wind-velocity appears twice in the upper part of the definition of the structure parameter (2.4). This term is the already known structure function D_w^2. The lower part of (2.4) is not influenced by the effects mentioned above. Therefore it is better to compute correction-factors for the 2-nd order structure functions. These factors can simply be applied to the structure parameters. We just want to avoid unneeded ballast in our equations and wish to make clear which part of the C_w^2-definition is influenced by the mentioned effects.

When the signal leaves the SONIC, it is sampled with a datalogger or computer. The exact timing of the computer sampling relative to SONIC sampling can have influence on

the correction. It is good to realize that the structure functions are computed in the computer, not in the SONIC.

In the calculation of the corrections we assume that the measured structure parameters lie in the isotropic part of the inertial subrange.Whether this assumption is valid or not, will be evaluated.

3.1 Measurement principle of the sonic anemometer

The sonic anemometer is a useful instrument for measurements of the three wind-velocity components. Especially the vertical component of the wind can be measured accurately, since the path between the transducers is oriented normal to the airflow. We look at a sonic anemometer, which determines wind-velocity from the difference between the reciprocal traveling-times of sound-pulses, transmitted in opposite directions across a fixed path. These pulsed sound waves have a frequency of 100 kHz. To measure one component of the wind, the SONIC needs two tranducers, directed towards each other, which act successively as transmitter and receiver. We focus our attention on the measurement of the vertical component of wind-velocity. A schematic picture is drawn to obtain clear insight into the measurement principle.

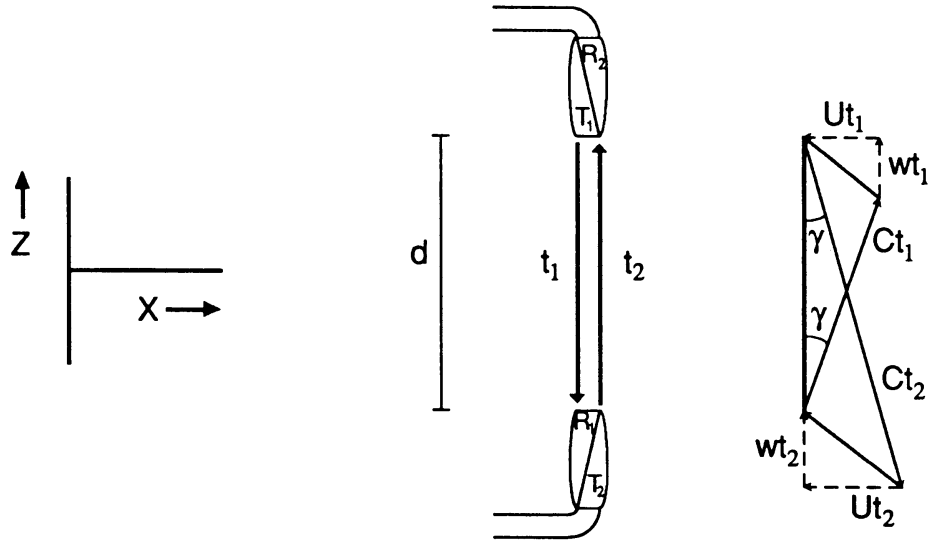

fig.3.1 Schematic presentation of the way in which the sonic anemometer measures vertical wind-velocity.

The symbols T and R stand for Transmitter and Receiver. The numbers accompanying these symbols denote the sequence of transmitting and receiving by the transducers. Before we derive the equations for the traveling-times, we realize that it is impossible to measure a velocity component at one point with a SONIC. As can be seen in figure 3.1 the vertical wind-speed (w) is averaged over a path with length d. The measured vertical wind is line-averaged ($\widetilde{w}$). Using the frame of reference of figure 3.1, we deduce:

$$\widetilde{w}(\vec{x}) = \frac{1}{d}\int_{-d/2}^{d/2} w(\vec{x}+z\vec{e}_z)\,dz \tag{3.1}$$

in which $\vec{x}$ indicates the middle of the path over which the vertical wind-speed is measured. Assuming an uniform wind and temperature field, we derive for the traveling-times upwards (t_u) and downwards (t_d) at time t:

$$\begin{aligned} t_u(t) &= \frac{d}{C\cos\gamma + \widetilde{w}(t)} \\ t_d(t) &= \frac{d}{C\cos\gamma - \widetilde{w}(t)} \end{aligned} \tag{3.2}$$

Here C is the velocity of sound in air. As can be seen in figure 3.1, $\gamma = \sin^{-1}\left(\frac{U}{C}\right)$, U is the horizontal wind-velocity. γ quantifies the deviation of the sound-path caused by the horizontal wind-component, mostly γ is very small: $O(10^{-2})$ rad. The transducers transmit their sound waves when they are triggered. This is always done in the same sequence: A^+, A^-, B^+, B^-, W^+, W^- (see figure 3.2). Concerning the vertical wind measurement we conclude that t_d is determined before t_u.

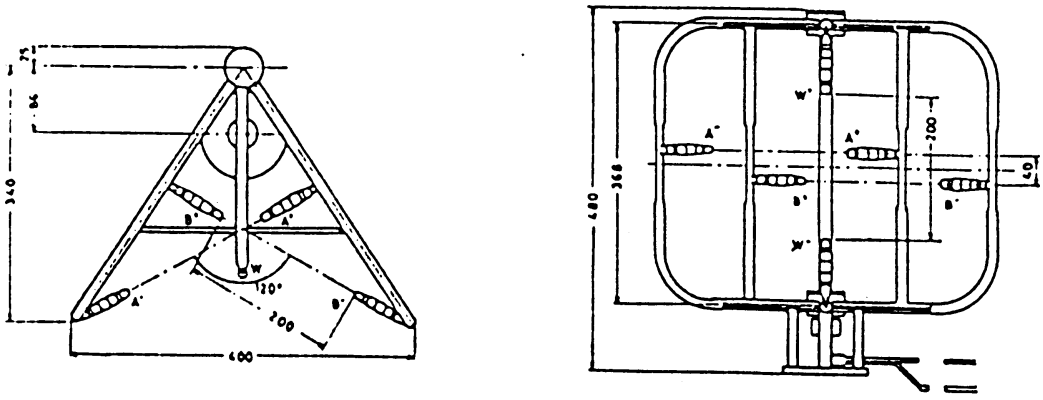

fig.3.2 The SONIC probe with labelled transducers (from Schotanus, 1982).

The time-interval between the triggering of W^+ and W^- is called t_m. From the SONIC specifications (Kaijo Denki) can be concluded that this time-interval is 1/6 of the total measurement cycle (t_r) in which all velocity components are measured. The latter is approximately 53.1 msec. The SONIC computes the vertical wind-velocity component, at time t, following

$$w_{comp} = \frac{d}{2}\left(\frac{1}{t_u(t)} - \frac{1}{t_d(t-t_m)}\right) = \frac{\tilde{w}(t) + \tilde{w}(t-t_m)}{2} \qquad (3.3)$$

From this equation is clear that what is really measured is an averaged value of two line-averaged vertical wind-speed values. This will affect the structure parameters. We did not count with some other effects, like the variation in C over t_m and the influence of time- averaging in $\tilde{w}(t)$ and $\tilde{w}(t-t_m)$, during the travel of the pulses. These effects are small and also diminish in the quadratic numerator of the C_w^2 definition.

3.2 Signal-handling of the SONIC DAT-300

In the previous section we looked at the way in which vertical velocity is measured by the SONIC. Now we look at the signal that holds the information. What happens to the signal, travelling from probe to computer?

This trip is visualized schematically in figure 3.3.

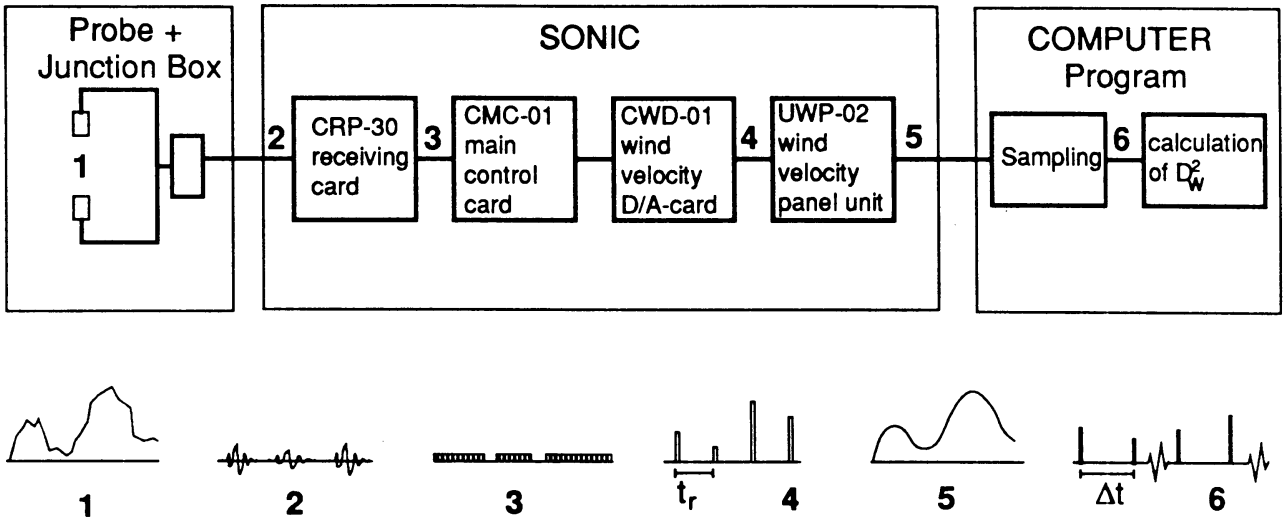

fig.3.3 Visualisation of the path to be followed by the vertical wind-velocity signal. Also the signal characteristics at several points lieing on this path.

The vertical velocity signal (1) is sampled, using up- and down-going sound-pulses, by the SONIC (2). This takes place at a sampling rate of approximately 20 times per second. The sample period is t_r. Next the inverse traveling-time of the sound-pulses is calculated by the receiving card, and that information is put in an digital pulse train (3). This train leaves the receiving card on its way to the main control card. The main control card does not affect the signal, it just puts it on the right channel. Soon afterwards the pulse train arrives at the wind-velocity D/A card. This card holds a counter that counts the pulses of the incoming train. It counts down for the first train, which holds information of $1/t_d$, and up for the next train ($1/t_u$). This all happens under control of the main control card. In this way the signal ($1/t_u$-$1/t_d$) is created, it is stored in pulses (4). This signal is then submitted to the wind-velocity panel unit. As far as known, this unit keeps the signal at the same value during t_r, and amplifies it dependent on the range in use. It may also contain a filter that removes the sharp edges of the block signal, but we read nothing about it in the specifications of the DAT-300.

At the end of the route through the SONIC the wind-speed signal leaves the SONIC and is sampled again at a different sample-rate (6) by the sampling programs which collect the data from the SONIC and compute D_w^2 and C_w^2.

To quantify the effect of the signal-handling, we follow the same path as the wind-speed signal. Starting point is the D/A-card, which computes the vertical wind-speed, as given by (3.3). The digitalizing of the travel-time signal, before the D/A-card does not seriously affect the signal. Digitalizing can only introduce an error caused by the rounding of the values to an integer number of pulses.

The samples of the vertical wind-speed, $w_s(t)$, are given by

$$w_s(t) = \sum_{i=-\infty}^{\infty} w_{comp}(it_r)\delta(t-it_r) \tag{3.4}$$

Here $\delta(t)$ is the delta function. Logically i is an integer variable.This signal (w_s) arrives at the wind-velocity panel unit. The effect of this unit can be described, using its impulse response-function h(t):

$$w_{out}(t) = h(t) * w_s(t) \tag{3.5}$$

The symbol * denotes continuous-time convolution (Oppenheim et al. 1983, p90). w_{out} is the resulting vertical wind-velocity that leaves the SONIC. h(t) depends on whether or not there is a filter in the unit. What is known from the specifications, is that the panel-unit holds a value until the next value arrives. So without filter h(t) can be described by

$$\begin{aligned} h(t) &= 1 \qquad 0 \le t < t_r \\ h(t) &= 0 \qquad t < 0 \vee t \ge t_r \end{aligned} \tag{3.6}$$

If there is a filter present in the panel unit, h(t) will have a form close to the above mentioned one. The total effect of the SONIC on the wind-velocity is obtained by combining (3.3), (3.4) and (3.5) into

$$w_{out}(t) = \sum_{i=-\infty}^{\infty} \left(\frac{\tilde{w}(it_r - t_m) + \tilde{w}(it_r)}{2} \right) h(t - it_r) \tag{3.7}$$

As mentioned above h(t) in not a completely unknown function. Although we are not certain about the precise form of h(t), we can conclude for every possible h(t) that h(t)= 0, t<0. This is because the SONIC system is a causal system. To make computation and interpretation of the correction easier, we suggest h(t)=0, for t>bt_r. Here b is an integer value which is greater than zero. Further we split t in two parts. A discreet part (a) and a small continu part (t'): t = at_r+t'. If the computer samples at time t, between qt_r and $(q+1)t_r$, then a=q and t'=t-qt_r. Thus t' has always a value between 0 and t_r.We can use the restrictions on h(t) combined with the split time to limit the summation of (3.7):

$$w_{out}(at_r + t') = \sum_{i=-b}^{0} \left(\frac{\tilde{w}([i+a]t_r - t_m) + \tilde{w}([i+a]t_r)}{2} \right) h(t' - it_r) \tag{3.8}$$

3.3 Calculation of the correction factors

We have derived a relation between the vertical velocity that leaves the SONIC, $w_{out}(t)$, and the real w(t). Now we can calculate the correction for use of the distorted $w_{out}(t)$ in the computation of D_w^2

With Taylor's Hypothesis (2.3) we write for $D_w^2(\Delta t)$, the structure function defined using time-variables:

$$D_w^2(\Delta t) = \left\langle \{ w(t) - w(t+\Delta t) \}^2 \right\rangle \tag{3.9}$$

From this equation it is clear that to calculate structure functions and their parameters the program which takes samples of the w_{out} data, needs measurements at time t and at time $t+\Delta t$.

Therefore we introduce Δ, the integer value that is the next upwards to the ratio $\left(\frac{\Delta t}{t_r}\right)$. The integer value Δ is needed because we use a sample at time $t+\Delta t$.

Before the expression for w_{out} is substituted in the defined structure function, it must be realized that the time averaging in equation (3.9) which can be written as an integral, changes due to the introduction of at_r+t'. If the averaging time $T=At_r$, then the brackets stand for $\frac{1}{At_r}\int_0^{At_r} dt$. In case of at_r+t' it becomes a combined summation over a and integration over t': $\frac{1}{A}\sum_{a=0}^{A-1} \frac{1}{t_r}\int_0^{t_r} dt'$. Substituting w_{out} in (3.9) with Δ yields:

$$D^2_{w_{out}}(\Delta t) = \left\langle \left\{ \sum_{i=-b}^{\Delta} \left(\frac{\tilde{w}([a+i]t_r - t_m) + \tilde{w}([a+i]t_r)}{2}\right)\left[h(t'-it_r) - h(t'+\Delta t - it_r)\right] \right\}^2 \right\rangle \qquad (3.10)$$

This expression can be worked out, however it is better to use a simplified notation for elaboration. Doing so will avoid many understanding problems concerning the way in which our correction is derived. We suggest the use of $w_i(a)$, short notation for the averaged value of two line-averaged vertical wind-speed values, obtained by the SONIC at $t=(a+i)t_r$:

$$w_i(a) = w_{comp}([a+i]t_r) = \left(\frac{\tilde{w}([a+i]t_r - t_m) + \tilde{w}([a+i]t_r)}{2}\right) \qquad (3.11)$$

And h_i, the term that brings the response-function in our correction:

$$h_i(t') = \left[h(t'-it_r) - h(t'+\Delta t - it_r)\right] \qquad (3.12)$$

The expression for $D^2_{w_{out}}(\Delta t)$ now becomes:

$$D^2_{w_{out}}(\Delta t) = \left\langle \left\{ \sum_{i=-b}^{\Delta} w_i h_i \right\}^2 \right\rangle \qquad (3.13)$$

Using w_i and h_i makes clear that we are dealing with a quadratic expression that can be evaluated without difficulties. Another integer variable, j, is needed to derive

$$D^2_{w_{out}}(\Delta t) = \left\langle \sum_{j=-b}^{\Delta} w_j w_j h_j h_j + 2\sum_{i=1}^{\Delta+b} \sum_{j=-b}^{\Delta-i} w_j w_{j+i} h_j h_{j+i} \right\rangle \tag{3.14}$$

As suggested above the brackets can be replaced by a summation over a and integration over t'. Equation (3.11) and (3.12) show that w_j depends on a and h_j on t', this yields:

$$\langle w_j w_{j+i} h_j h_{j+i} \rangle = \frac{1}{A}\sum_{a=0}^{A-1} w_j(a) w_{j+i}(a) \; \frac{1}{t_r}\int_0^{t_r} h_j(t') h_{j+i}(t')\, dt' \tag{3.15}$$

Because we use half hour averages, A is big in our case. Therefore we state that the summation approximates the time averaged $\langle w_j w_{j+i} \rangle$. Further we assume that this part of the expression above is only dependent on the difference between j and j+i, thus:

$$\frac{1}{A}\sum_{a=0}^{A-1} w_j(a) w_{j+i}(a) = \langle w_j w_{j+i} \rangle = F_w(i) \tag{3.16}$$

The validation of this assumption will be given when we evaluate $F_w(i)$. The two equations above filled in (3.14) give:

$$D^2_{w_{out}}(\Delta t) = F_w(0)\sum_{j=-b}^{\Delta} \langle h_j h_j \rangle_{t_r} + 2\sum_{i=1}^{\Delta+b} F_w(i) \sum_{j=-b}^{\Delta-i} \langle h_j h_{j+i} \rangle_{t_r} \tag{3.17}$$

Here $\langle \; \rangle_{t_r}$ means that the inner has to be averaged over t_r. To obtain a clear expression that describes the relation between the structure function which is measured, and the real $D^2_w(\Delta t)$, a function is introduced. This function, $I_{resp}(i)$, is closely related to the response-function h(t):

$$I_{resp}(i) = \sum_{j=-b}^{\Delta-i} \langle h_j h_{j+i} \rangle_{t_r} \tag{3.18}$$

Substitution of I_{resp} in (3.17) then gives the equation that is taken as basis for the derivation of the correction:

$$D^2_{w_{out}}(\Delta t) = F_w(0)I_{resp}(0) + 2\sum_{i=1}^{\Delta+b} F_w(i)I_{resp}(i) \qquad (3.19)$$

In the next paragraph we work out $I_{resp}(i)$ to make this term computable. After that the derivation of the relation between $F_w(i)$ and $D^2_w(\Delta t)$ is given in paragraph 3.3.2.

3.3.1 Evaluation of the response term

In the previous section a short definition of I_{resp} was given. We write it out here, using the dimensionless time-variables $\tau = \frac{t'}{t_r}$ and $\Delta\tau = \frac{\Delta t}{t_r}$. The first time-variable, τ, denotes the position of the first program sample in the time-interval between two successive SONIC measurement-samples. We have taken the last SONIC sample (at $t=at_r$) before the program sample as zero-point of our time-axis, so τ has always a value between 0 and 1. $\Delta\tau$ stands for the dimensionless time between the two program samples. Figure 3.4 shows the relation between the moving time-axis used in our computations, and the real time-axis.

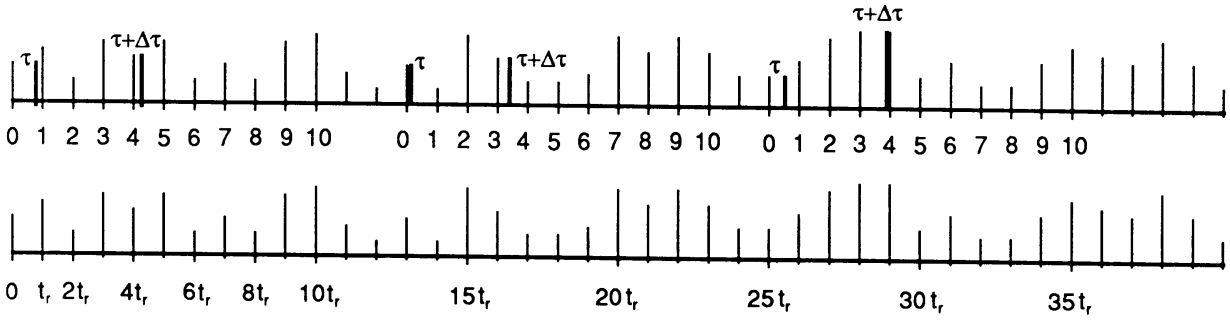

fig.3.4 Comparison of the dimensionless, moving time-axis with the real time-axis. Also visualisation a time-serie of the sonic sample moments (thin lines) and the program sample moments.(fat lines)

We also introduce $H(\tau)=h(t')$ to obtain a eqation for $I_{resp}(i,\Delta\tau)$, which is equal to $I_{resp}(i)$, but defined using dimensionless time-variables.

$$I_{resp}(i,\Delta\tau) = \sum_{j=-b}^{\Delta-i} \left\langle [H(\tau-j)-H(\tau+\Delta\tau-j)][H(\tau-j-i)-H(\tau+\Delta\tau-j-i)] \right\rangle_1 \qquad (3.20)$$

How do we evaluate the brackets enclosing the right-hand part of the expression above? The only varying time-variable is τ, which takes a different value each time the program takes a pair of measurements from the SONIC. The sampling program and the SONIC use different clocks for their timing. Therefore we suggest that τ is a stochastic variable with relative frequency distribution $k(\tau)$, $0\leq\tau<1$. This distribution function depends on the sampling program, whether it is triggered in some way by the SONIC or not. Using $k(\tau)$ we can replace the brackets of (3.20) by an integral between 0 and 1, which is in agreement with equation (3.15) because $\tau = \frac{t'}{t_r}$.

$$I_{resp}(i,\Delta\tau) = \sum_{j=-b}^{\Delta-i} \int_0^1 k(\tau)[H(\tau-j)-H(\tau+\Delta\tau-j)][H(\tau-j-i)-H(\tau+\Delta\tau-j-i)]\, d\tau \qquad (3.21)$$

In our case the program is not triggered in any way by the SONIC. It has its own timing circuit. Therefore we suggest that $k(\tau)$ takes the form of the uniform distribution function. Thus $k(\tau)=1$, $0\leq\tau<1$. This means that within the averaging-time there is equal chance of finding the moment of sampling by the sampling program in the interval between two succesive sample moments of the SONIC. This assumption about $k(\tau)$ simplifies the calculation of I_{resp}. We simply erase $k(\tau)$ in (3.21) and then execute a translation $\tau'=\tau-j$, which results in:

$$I_{resp}(i,\Delta\tau) = \sum_{j=-b}^{\Delta-i} \int_{-j}^{-j+1} [H(\tau')-H(\tau'+\Delta\tau)][H(\tau'-i)-H(\tau'+\Delta\tau-i)]\, d\tau' \qquad (3.22)$$

Combination of summation and integration is possible. The resulting integral is split in four parts:

$$I_{resp}(i,\Delta\tau) = \int_{i-\Delta}^{b+1} H(\tau')H(\tau'-i)\,d\tau' - \int_{i-\Delta}^{b+1} H(\tau')H(\tau'+\Delta\tau-i)\,d\tau' - \int_{i-\Delta}^{b+1} H(\tau'+\Delta\tau)H(\tau'-i)\,d\tau' + \int_{i-\Delta}^{b+1} H(\tau'+\Delta\tau)H(\tau'+\Delta\tau-i)\,d\tau' \quad (3.23)$$

The two integrals with the term $H(\tau'+\Delta\tau)$ are translated backwards over $\Delta\tau$. Every integral then contains the term $H(\tau')$. We suggested for h(t) that $h(t)=0,\ t<0,t>bt_r$. So $H(\tau')$ is equal to zero outside the interval $0\leq\tau'<b$. Clealy 0 and b are safe limits for all our integrals in (3.23). Now these four can be combined in one, this yields:

$$I_{resp}(i,\Delta\tau) = \int_{0}^{b} H(\tau')\left[2H(\tau'-i) - H(\tau'-\Delta\tau-i) - H(\tau'+\Delta\tau-i)\right] d\tau' \quad (3.24)$$

With any known h(t), it is simple to compute I_{resp}, using the equation above.

3.3.2 Influence of line-averaging

The evaluation of F_w is important because it brings D_w^2, the real structure function, back in our equations. And that function is the one we want to have available. The first step to attain this is to fill the expression for w_i (3.11) in $F_w(i)$ (3.16), and subsequently split the obtained relation in four parts:

$$F_w(i) = \frac{1}{4}\left\langle \tilde{w}([a+j]t_r-t_m)\cdot \tilde{w}([a+j+i]t_r-t_m)\right\rangle + \frac{1}{4}\left\langle \tilde{w}([a+j]t_r-t_m)\cdot \tilde{w}([a+j+i]t_r)\right\rangle + \frac{1}{4}\left\langle \tilde{w}([a+j]t_r)\cdot \tilde{w}([a+j+i]t_r-t_m)\right\rangle + \frac{1}{4}\left\langle \tilde{w}([a+j]t_r)\cdot \tilde{w}([a+j+i]t_r)\right\rangle \quad (3.25)$$

This expression let us deal four times with the term $\left\langle \tilde{w}(t_1)\cdot \tilde{w}(t_2)\right\rangle$, in which t_1 and t_2 denote two points in time. This term can easily be related to $\left\langle \tilde{w}(x_1\vec{e}_x)\cdot \tilde{w}(x_2\vec{e}_x)\right\rangle$ with

Taylors hypothesis. Using the expression for the line-averaged vertical velocity (3.1) we work it out:

$$\langle \tilde{w}_1 \cdot \tilde{w}_2 \rangle = \frac{1}{d^2} \left\langle \int_{-d/2}^{d/2} w(x_1 \vec{e}_x + z\vec{e}_z)\, dz \cdot \int_{-d/2}^{d/2} w(x_2 \vec{e}_x + z\vec{e}_z)\, dz \right\rangle \qquad (3.26)$$

Here $\langle \tilde{w}_1 \cdot \tilde{w}_2 \rangle$ is an abbreviation for $\langle \tilde{w}(x_1\vec{e}_x) \cdot \tilde{w}(x_2\vec{e}_x) \rangle$. The expression above can be elaborated with use of the correlation tensor R_{ij} that is related to the velocity $\vec{u}$ in two points, $\vec{r}_1$ and $\vec{r}_2$ (Nieuwstadt,1989)

$$R_{ij}(\vec{r}_1 - \vec{r}_2) = \langle u_i(\vec{r}_1) \cdot u_j(\vec{r}_2) \rangle \qquad (3.27)$$

in which u_i denotes the i-th component of $\vec{u}$. The third component of this vector is w. The assumption of isotropy, earlier stated, happens to produce important effects at the third component of R_{ij}: R_{33}. In the case of isotropy the structure of turbulence can be described totally by two scalar functions. These functions, f and g, separate R_{33} in respectively a longitudinal and a transversal component (Nieuwstadt, 1989); (Hinze, 1957).

$$R_{33}(r) = \{f(r) - g(r)\}\frac{r_3^2}{r^2} + g(r) \qquad (3.28)$$

in which r_3 is the third component of $\vec{r}$. Further it can be derived for f and g:

$$r\frac{\partial f(r)}{\partial r} + 2\{f(r) - g(r)\} = 0 \qquad (3.29)$$

It is clear that $R_{33}(0) = \sigma_w^2$, the variance of the vertical wind-speed, and thus we obtain from (3.28): $g(0) = \sigma_w^2$. Recollect that the structure parameters relate to the inertial subrange. We use the modified similarity theory to estimate the right form of g(r) and with (3.29) for f(r):

$$g(r) = \sigma_w^2 - C^* l^{\mu_{2/3}} \varepsilon^{2/3} r^{2/3-\mu_{2/3}}$$
$$f(r) = \sigma_w^2 - 0.75 C^* l^{\mu_{2/3}} \varepsilon^{2/3} r^{2/3-\mu_{2/3}} \tag{3.30}$$

Here C^* is a non-absolute constant as in equation (2.10).

We can substitute (3.27) in (3.26), this yields:

$$\langle \tilde{w}_1 \cdot \tilde{w}_2 \rangle = \frac{1}{d^2} \int_{-d/2}^{d/2} \int R_{33}\left[(x_1 - x_2)\vec{e}_x + (z - z')\vec{e}_z\right] dz dz' \tag{3.31}$$

Due to the line-averaging that took place twice, an extra parameter z' arises and the two line-integrals transform into a surface integral. Due to translation invariance (equation 3.26) we can convert the right part of (3.31) back into a line integral with $\zeta = z - z'$

$$\langle \tilde{w}_1 \cdot \tilde{w}_2 \rangle = \frac{1}{d} \int_{-d}^{d} R_{33}\left[(x_1 - x_2)\vec{e}_x + \zeta \vec{e}_z\right]\left(1 - \frac{|\zeta|}{d}\right) d\zeta \tag{3.32}$$

With the equations for f and g, R_{33} becomes

$$R_{33}(r) = \sigma_w^2 - \left(1 - \frac{1}{4}\frac{r_3^2}{r^2}\right) C^* l^{\mu_{2/3}} \varepsilon^{2/3} r^{2/3-\mu_{2/3}} \tag{3.33}$$

This expression for R_{33} can directly be substituted in (3.32). We also use $y = \frac{|\zeta|}{d}$ to rewrite the integral

$$\langle \tilde{w}_1 \cdot \tilde{w}_2 \rangle = 2 \int_0^1 \left\{ \sigma_w^2 - C^* l^{\mu_{2/3}} \varepsilon^{2/3} d^{2/3-\mu_{2/3}} \left[\left(\frac{x_1 - x_2}{d}\right)^2 + \frac{3}{4} y^2\right]\left[\left(\frac{x_1 - x_2}{d}\right)^2 + y^2\right]^{-2/3 - 1/2\mu_{2/3}} \right\} (1 - y) dy \tag{3.34}$$

We can relate $\langle \tilde{w}_1 \cdot \tilde{w}_2 \rangle$ and the structure function which is not influenced by the SONIC, $D_w^2(\Delta x)$, by deriving for the latter:

$$D_w^2(\Delta x) = 2[R_{33}(0) - R_{33}(\Delta x \vec{e}_x)] = 2C^* 1^{\mu_{2/3}} \varepsilon^{2/3} \Delta x^{2/3 - \mu_{2/3}} \tag{3.35}$$

To simplify the resulting expression we define an integral-function: $I_{line}(x)$, that is used to take line-averaging into account.

$$I_{line}(x) = \int_0^1 \left(x^2 + \frac{3}{4}y^2\right)(x^2+y^2)^{-2/3 - 1/2\mu_{2/3}}(1-y)dy \tag{3.36}$$

Finally we obtain from (3.34) the relation between $\langle \tilde{w}(t_1) \cdot \tilde{w}(t_2) \rangle$ and $D_w^2(\Delta t)$ using Taylors hypothesis (2.3), I_{line} and (3.35).

$$\langle \tilde{w}(t_1) \cdot \tilde{w}(t_2) \rangle = \sigma_w^2 - \left(\frac{d}{U\Delta t}\right)^{2/3 - \mu_{2/3}} I_{line}\left(\frac{U(t_2 - t_1)}{d}\right) D_w^2(\Delta t) \tag{3.37}$$

We substitute this equation in (3.25) to obtain the relation between $F_w(i)$ and $D_w^2(\Delta t)$. The assumption $\langle w_j w_{j+i} \rangle = F_w(i)$ appears to be valid because we have no terms depending on j left. Two dimensionless variables are introduced in order to get an understandeble result: $r = \frac{U t_r}{d}$, and $m = \frac{U t_m}{d}$. Here r is the distance over which the air is displaced in the time interval t_r, made dimensionless with d, the distance between the transducers in the SONIC-frame. Further m is the distance over which the air is displaced in the time-interval t_m. We obtain for $F_w(i)$:

$$F_w(i) = \sigma_w^2 - \frac{1}{2}\left(\frac{d}{U\Delta t}\right)^{2/3 - \mu_{2/3}} D_w^2(\Delta t)\left\{\frac{1}{2} I_{line}(ir-m) + I_{line}(ir) + \frac{1}{2} I_{line}(ir+m)\right\} \tag{3.38}$$

Substitution of this expression in (3.19) and rearranging the resulting equation leads to the correction we were looking for:

$$D_{w_{out}}^2(\Delta t) = N_{corr}\sigma_w^2 + F_{corr} D_w^2(\Delta t) \tag{3.39}$$

In this equation N_{corr} is defined by:

$$N_{corr} = I_{resp}(0,\Delta\tau) + 2\sum_{i=1}^{\Delta+b} I_{resp}(i,\Delta\tau) \tag{3.40}$$

And F_{corr} is defined by:

$$F_{corr} = -\frac{1}{2}\left(\frac{d}{U\Delta t}\right)^{2/3-\mu_{2/3}} \left\{ \begin{array}{l} [\, I_{line}(0)+I_{line}(m)\,]I_{resp}(0,\Delta\tau) + \\ \quad 2\sum_{i=1}^{\Delta+b} \left[\frac{1}{2}I_{line}(ri-m)+I_{line}(ri)+\frac{1}{2}I_{line}(ri+m) \right] I_{resp}(i,\Delta\tau) \end{array} \right\} \tag{3.41}$$

Finally we are left with a well computable correction for the structure functions measured by the SONIC. We rewrite (3.39) for the structure parameters by dividing it by $(U\Delta t)^{2/3}$, and subsequently rearranging results in:

$$C_w^2(\Delta t) = \frac{C_{w_{out}}^2(\Delta t)}{F_{corr}} - \frac{N_{corr}}{F_{corr}} \frac{\sigma_w^2}{(U\Delta t)^{2/3}} \tag{3.42}$$

The second term on the right side of this equation can cause negative structure parameters when the first term is small. We prefer a correction for which N_{corr} is zero, so we can also correct small structure parameters.

4 MEASUREMENTS OF THE STRUCTURE PARAMETER AT THREE SITES

To check the correction, derived in the previous chapter and to obtain some scaling relations for the vertical structure parameter, measurements were used obtained in the period of 1987 till 1989. Time-series of the structure parameter of vertical velocity were recorded under different circumstances at three sites, two of them in the Netherlands (SPEULD and CABAUW) and one in France (CRAU). A brief description of the sites and the field-experiments is given in paragraph 4.1, 4.2 and 4.3. At all sites structure parameters have been measured with varying time-intervals. The intervals in use are: 0.04, 0.08, 0.16 and 0.32 seconds (all multiples of the net frequency to reduce noise interference). We call the structure parameters relating to these time-intervals respectively: Cww1, Cww2, Cww4 and Cww8. If the structure parameters lie in the inertial subrange, the ones measured at the same time over a different interval should have the same value. (see §2.3) This is an useful feature which allows us to check our correction. Moreover we can choose which structure parameter (1, 2, 4 or 8) is the best to use for analyses. For each dataset the mean of the length of the wind-vector (U) is computed. This is a corrected version of the common used wind vector (FFSN), see appendix A1.

4.1 Crau

In june 1987 an experiment took place in Crau. Several institutes from different countries coöperated in this experiment. We use the data resulting from the KNMI-contribution (Kohsiek et al. 1988).

Crau is a dry and flat area, situated in the south of France. The terrain surrounding the KNMI measurement station is rather homogeneous, covered with pebbles, small stones, and sparse vegetation. Of interest are the data collected from the sonic anemometer in use. This was a Kaijo Denki DAT-300 with sensor TR61A. The SONIC was placed in a mast at 11.35 meter. It was turned towards the mean wind direction by

hand. Of course this action is not error-free: the difference between the SONIC direction and the mean wind direction was often more than 20 degrees. Therefore we performed an azimuth correction on the mean wind and the friction velocity (u_*) (see Appendix A1). Another correction which has been applied to u_* is the one for tilting (Duyzer and Bosveld, 1988). This is a correction for flow-blocking obstacles underneath the SONIC frame (Appendix A1). The correction of u_* carries over in L, so we also put a corrected version of L in the Crau-dataset. This all is done with the programs CRAUCOR and LOEDCOR, they are listed in appendix B2. In Crau the time-intervals 0.04, 0.08 and 0.16 were used to compute the structure parameters Cww1, Cww2 and Cww4.

4.2 Speuld

The second place that we use, at which measurements of the structure parameter of vertical wind-velocity were obtained, is in the Netherlands. These measurements were performed within the research program ACIFORN. The Speulderbos is located 2 km north of the village Garderen, 20 kilometres west of the city Apeldoorn. It contains a Douglas fir stand above which our measurements were obtained. Trees are between 15 and 20 m tall. Bosveld (1995)gives a description of the surroundings and the mast in which the sonic anemometer (type Kaijo Denki DAT-300, probe TR-61A) is placed. The measurement height of the sonic anemometer is 29.7 metres, this is the height measured from the ground-level. To obtain the real measurement height, relative to the fir stand, we have to substract the displacement height, which is 12.5 metres. Thus relative to the displacement height, structure parameters were measured at 17.2 metres measurement height.

For the data of SPEULD the same corrections of U and u_* were needed as for CRAU. The corrected version of u_* was already present in the dataset. U is corrected and placed in the dataset with the program USPEULD (see Appendix B3) Due to mast interference, we had to exclude the wind-direction from 300 uptill 30 degrees.

In this range the ratio of the structure parameters show a clear increase (see figure 4.1).

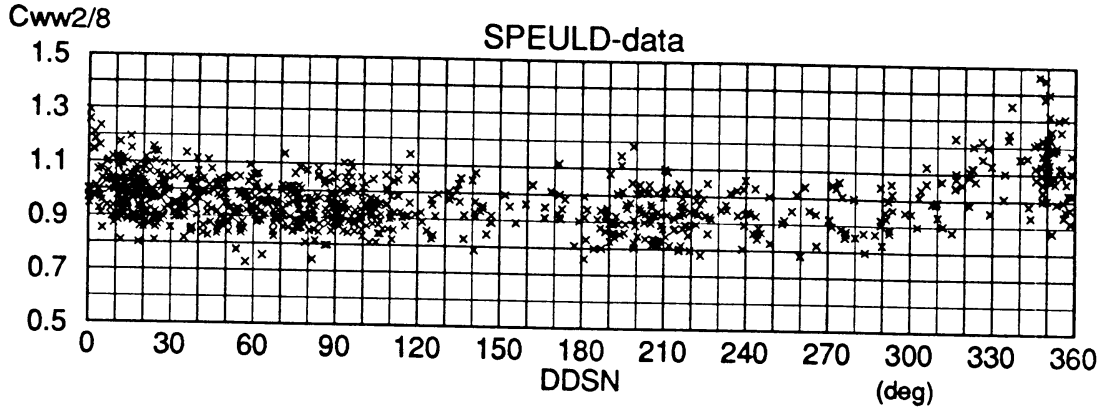

fig 4.1 Influence of the wind-direction on the structure parameter ratio for Speuld.

The sampling program in SPEULD uses the time-intervals 0.08, 0.16 and 0.32 for the computation of the structure parameters. We use data measured in the month May, 1989, out of this large dataset.

4.3 Cabauw

The last time-series of C_w^2 measurements which we use, were obtained in the period July the 24th till October the 7th, 1989, during an experiment about flux-profile relationship in the nocturnal boundary layer (Bouwman, 1990). A mast with a sonic anemometer was situated 120 m north west from the 213 m meteorological mast in Cabauw. The type SONIC was again Kaijo Denki DAT-300 with probe TR-61A. It was replaced once during the experiment by another sonic anemometer of the same type. The center of the SONIC was 11.4 metres above the ground. The terrain surrounding the measurement-mast can be divided into sectors, with different grade of inhomogenity (Bouwman, 1990).

Just like at SPEULD, we see a rising Cww's ratio for a special sector, this time for the sector 110-180 degrees (see figure 4.2). This is caused by the main mast, we excluded this region. Monna and van der Vliet (1987) give a detailed description of the site.

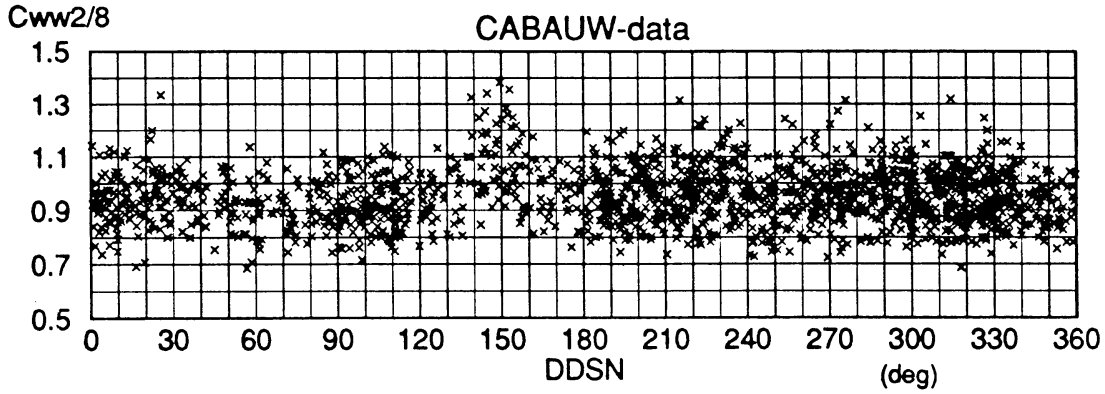

fig 4.2 Influence of the wind-direction on the structure parameter ratio for Cabauw.

A remarkable distinction with the two experiments before is the use of a program that turns the SONIC automatically into the mean wind direction every 10 minutes. Therefore we don't have to correct the measurements of U and u_* for the difference between the SONIC orientation and the mean wind direction. We excluded the measurements when the automatic rotator failed to do his job (See figure 4.3). The maximum difference is taken 20 degrees, so we have not much distortion of the wind field (<5%) by the frame of the SONIC (Schotanus 1982).

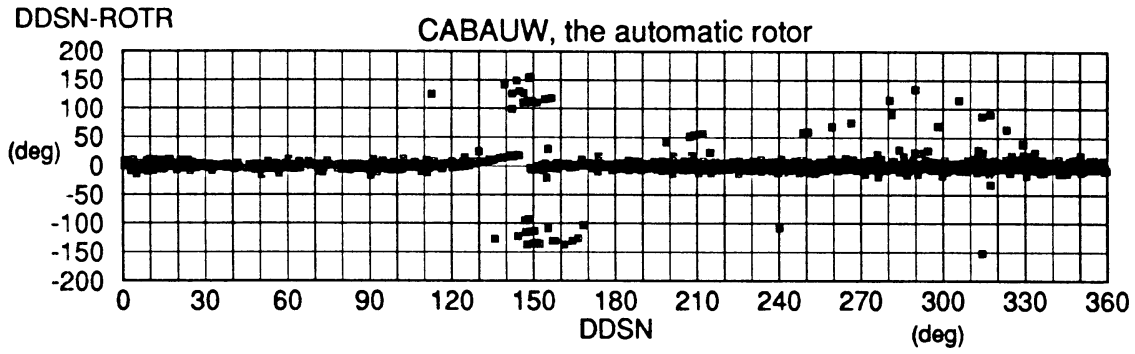

fig 4.3 Functioning of the automatic rotor in Cabauw.

The correction for tilting had still to be included. During the first attempt to do this,

problems occured concerning the dataset contents and description. Bouwman (1990) should have computed the USON component of the mean wind measured by the SONIC in the east direction, and the VSON component in the north direction. Comparison with the wind-direction at 10 m yields that USON was directed west-wards and VSON south-wards. This is corrected, also for <UW>, <VW>, <US>, <UT>, <VS>, <VT>. Further the wind-direction computed from the SONIC data (DDSN) is added, and FFSN, the SONIC wind speed. u_* and L were not available so they were computed in exactly the same way as Bouwman did, we only used a corrected version of u_*. In appendix B4 the two programs (CABCOR and LOBH) which execute these computations are listed. The program CWWSCABA was used to compute structure parameters out of the square root of the structure functions, which were available in the CABAUW dataset.

An important difference concerning the sampling program used in CRAU and SPEULD is that the sampling program of CABAUW has a fixed sample rate with a period of 0.8 seconds. In CRAU and SPEULD this period is varying around a mean value, dependent on the business of the computer. Finally we note that the structure parameters in CABAUW were obtained over the time-intervals 0.08, 0.16 and 0.32 seconds, which is the same as for the SPEULD dataset.

4.4 Data-handling

In this study we used datasets created and described by other investigators. We worked with 30-minute averaged values. The datasets have the extension B30, the correction programs mentioned above create datafiles with the extension C30. In appendix A3 the description files of the modified datasets are printed.

In order to deal with continuous turbulence we used selection criteria for the mean wind-velocity and friction velocity:

- $U > 2$ m/s
- $u^* > 0.15$ m/s

Next to these criteria only measurements were used for which

- $C_w^2 > 0.015\ m^{4/3}s^{-2}$

in order to avoid domination of the noise in C_w^2. Also periods of rain were excluded from our data files.

To correct the structure parameter of vertical wind-velocity 3 programs were used: IINTBER, IRESPBER and CORRECT. They are listed in appendix B1. The program that produces the correction factors N_{corr} and F_{corr} is 'CORRECT'. CORRECT uses the output of IINTBER and IRESPBER. IINTBER computes the integral I_{line} for a chosen interval. IRESPBER computes the necessary values of I_{resp} for a sudden responsfunction. The only information that is needed by CORRECT next to these two components of F_{corr} and N_{corr} is a file with wind-speed data. With all this information CORRECT produces a file with correction-factors for Cww1, 2, 4 and 8. The measurement data was imported in the spreadsheet program LOTUS together with the correction factors. In LOTUS the structure parameter data were corrected.

5 RESULTS

We wanted to obtain good measurements of the structure parameter of vertical velocity in the inertial subrange. With that purpose a correction was computed. This is done with the assumption that the structure parameters lie in the isotropic inertial subrange. In paragraph 5.1 this assumption is evaluated for the three datasets we use. In the next paragraph several correction functions, obtained with different impuls response functions are compared with each other. The exact impuls-respons function is still not known, so we choose the most likely function. Then the results of the correction applied to the different structure parameters at the three sites, are given in paragraph 5.3 Some scaling relations for C_w^2 are given in the last part of this chapter.

5.1 Inertial subrange limits

As explained in §2.1 we take the ratio of two structure parameters, measured over a different interval as indicator of the inertial subrange limits. We plot the ratio against z/D, D=2UΔt. Here D is the size of the eddy we're looking at, because the maximum response from the structure parameter is given by an eddy which size is twice the space-interval over which the structure parameter is measured.

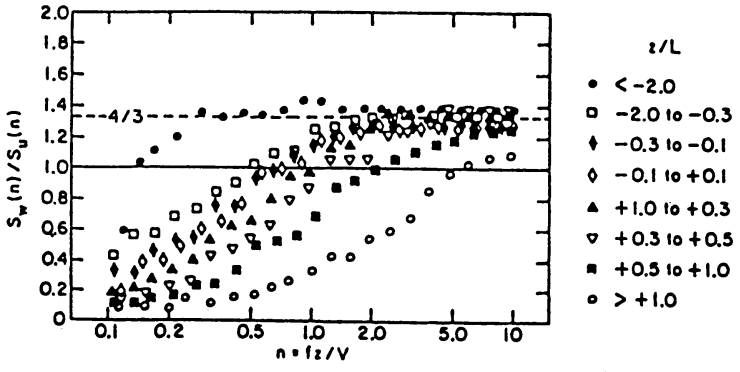

fig 5.1 Plot of the ratios of w and u spectral estimates, from Kaimal et al.(1972)

The ratio z/D can be compared with the dimensionless frequency which Kaimal et al.

(1972) use in their plot to verify isotropy, see figure 5.1. In this plot is f the frequency which can be compared with $1/2\Delta t$ from the C_w^2 definition.

We use the corrected structure parameters for the ratios.

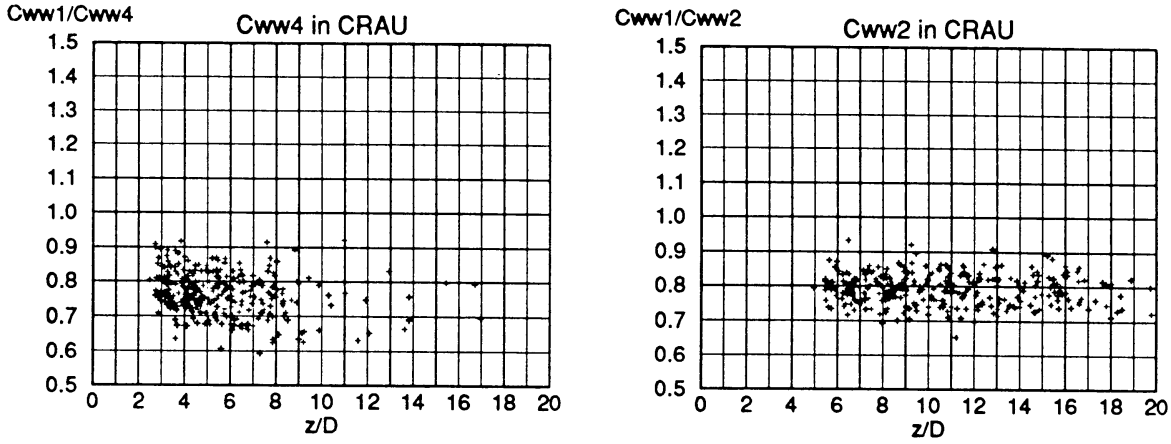

fig 5.2 Cww's ratios in Crau start to rise at z/D=5, then they are no longer in the inertial subrange.

For Crau we see (fig 5.2) that the ratio Cww1/4 begins to rise at z/D =5. The ratio Cww1/2 does not rise at all. Thus we are sure that the structure parameters behave as expected in the inertial subrange for z/D >5. The same can be concluded from figure 5.3: Cww8 does not show inertial subrange behaviour in Cabauw for z/D too low. In Speuld Cww8 stays in the inertial subrange.

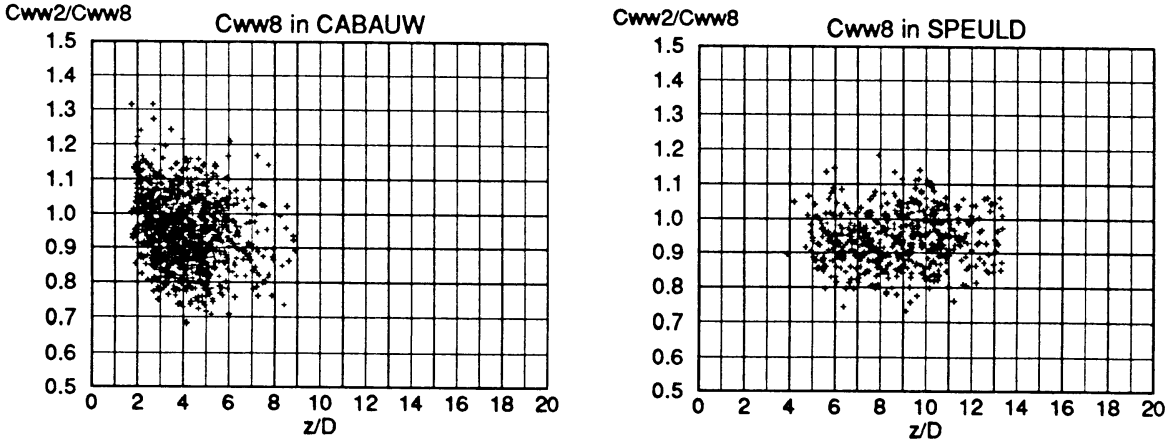

fig 5.3 Cww's ratios in Cabauw and Speuld, limits of the inertial subrange are reached.

Now we can decide which intervals we use for further analyzing of the data measured at the different sites. These are the intervals for which C_w^2 is in the inertial subrange.

Site	Interval	Struc.Parameter
Crau	0.04, 0.08	Cww1, Cww2
Speuld	0.08, 0.16, 0.32	Cww2, Cww4, Cww8
Cabauw	0.08, 0.16	Cww2, Cww4

table 5.1. The possible intervals for the structure parameters to be sure they lie in the inertial subrange.

In figure 5.4 we split the data of figure 5.3a in six stability categories, the same as used in figure 5.1. We only plotted averaged values for the structure parameter ratio. Under stable conditions, the ratio starts to rise earlier, at z/D=6; in the unstable case at z/D=3.

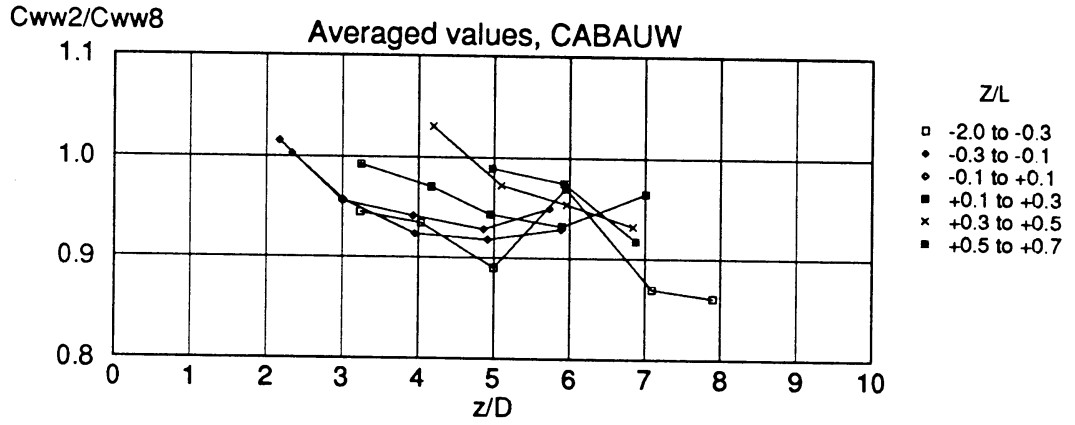

fig 5.4 The Cabauw data split in several stability categories, averaged values are plotted to show the stability dependence of the limits.

This is in agreement with figure 5.1, in which the spectral ratio begins to sink earlier for stable categories. Kaimal et al. tested for isotropy via the 4/3-condition mentioned in §2.1 That the figure they obtained (fig. 5.1) can well be compared with figure 5.4, in which a C_w^2-ratio test is visualized, supports the opinion that this test is indeed a test for isotropy.

5.2 Correction factors of different response-functions

We do not know the exact impulse-response function of the SONIC. What we know about it is written in §3.2. Without a filter that removes sharp edges, h(t) (and thus H(τ)) should be shaped as H1 in figure 5.5. This is a rather ideal function, therefore we computed correction factors for 3 variations on H1. These are also plotted in figure 5.5.

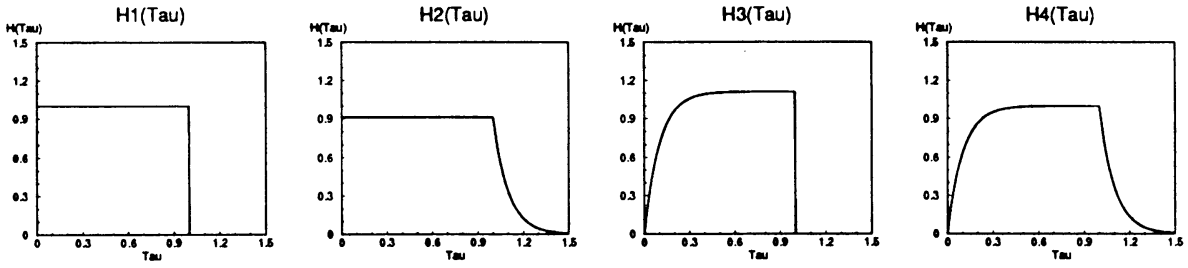

fig 5.5 The tested impulse-response functions.

The functions are defined in Table 5.2. The multiplying factors result from the restriction that $\int_0^\infty h(t)\,dt = 1$. The results of the computations are plotted in figure 5.6 (F_{corr}) and listed in table 5.2 (N_{corr}). For each function four F_{corr}-curves are plotted, for the four different intervals of the structure parameters. The lowest curve is for Cww1, then Cww2, Cww4 and the highest is for Cww8.

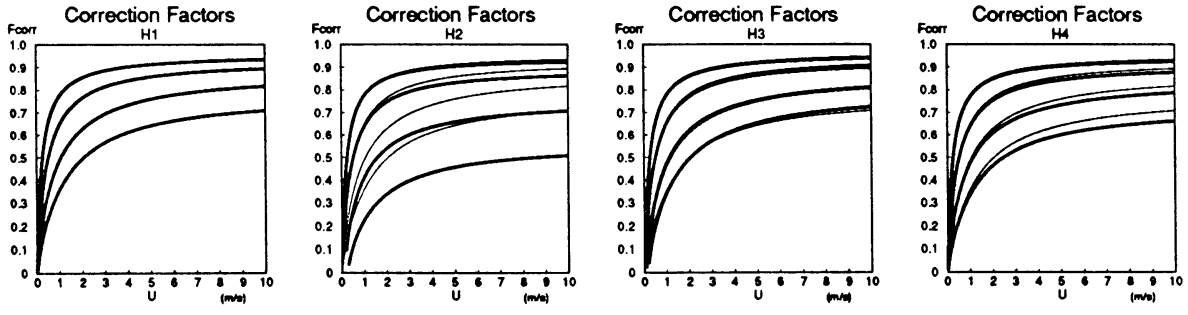

fig 5.6 F_{corr} curves for the four tested functions.

H2 changes a lot: The F_{corr} curves lie appreciable lower for Cww1 and Cww2. But the N_{corr} factors increase, which is far from ideal. This function is not very realistic, because it starts at one for $\tau=0$.

The F_{corr}-curves produced by H3 are equal to that of H1 within a few percent. N_{corr}1,2,4 and 8 are even greater than for H2. H3 is also not realistic, stopping at ones for τ=1.

The last variation on H1, H4, produced surprisingly N_{corr} factors that are equal to zero! The F_{corr} curves differ a bit, but not very seriously. H4 is a realistic function, having a negative e-exponent at start and end. Such an exponent is often produced by a RC-circuit. We chose a factor 10 as muliplication factor in the e-exponent, this factor is a acceptable value for a realistic filter.

	$0 \leq \tau < 1$	$1 \leq \tau$	$N_{corr}1$	$N_{corr}2$	$N_{corr}4$	$N_{corr}8$
H1(τ)	1	0	0	0	0	0
H2(τ)	0.909	$0.909e^{-10(\tau-1)}$	0.074	0.081	0.008	0.018
H3(τ)	$1.111(1-e^{-10\tau})$	0	0.113	0.122	0.015	0.028
H4(τ)	$1-e^{-10\tau}$	$e^{-10(\tau-1)}$	0	0	0	0

table 5.2 Definition of H1,H2,H3 and H4. Also the computed Ncorr factors.

Because the deviation from the ideal F_{corr}-curves is within 5 percent for Cww2,4,8 and we cannot be sure of the factor in the e-exponent, we choose the ideal H1 as our correction function. Regarding the correction (F-)curves we now can choose which interval is the best to use in further analysis for the separate measurement places. The best is the one which needs the minimum correction, thus the highest possible curve. This highest curve relates to the biggest space-interval. Therefore we conclude with use of table 5.1:

Site	Interval	Struc.Parameter
Crau	0.08	Cww2
Speuld	0.32	Cww8
Cabauw	0.16	Cww4

table 5.3. The chosen intervals for the best structure parameters to use.

5.3 Correction of the measurements

For the evaluation of our correction done with function H1(t), we used again ratios of structure parameters, measured over a different interval. In §5.1 they appear to be sensible indicators. As expressed in equation (2.15), these ratios can't reach unity. Using $\mu_{2/3} = -0.05$ results in the following values for the ratios:

$$Cww1/Cww4 = Cww2/Cww8 \approx 0.93$$

$$Cww1/Cww2 = Cww2/Cww4 = Cww4/Cww8 \approx 0.97$$

In figure 5.7 the ratios Cww1/4 and Cww1/2 stay too low; Cww2/4 is quite good. In figure 5.7a and b the ratios increase for growing Cww4. Remember that for windspeeds greater than 7 m/s in Crau, Cww4 leaves the inertial subrange. It is remarkable that the deviation of the structure parameter ratio is within 10 percent even for low values of the structure parameters.

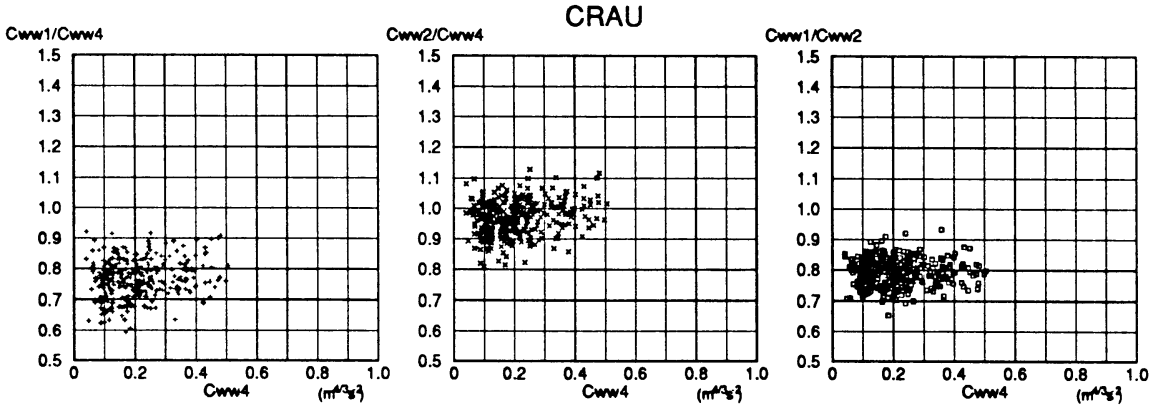

fig 5.7 Ratios of the structure parameter of vertical wind-velocity in Crau.

In the Speuld-data, some outliers are present in the Cww2/8 ratio. The cause of these outliers couldn't be detected. In this dataset we see a deviation for small Cww's: the ratio seems to fluctuate some more. The ratios Cww2/8 and Cww2/4 (figure 5.8) take the expected value. The ratio Cww4/8 becomes to high, not much (3%), but it is determinable.

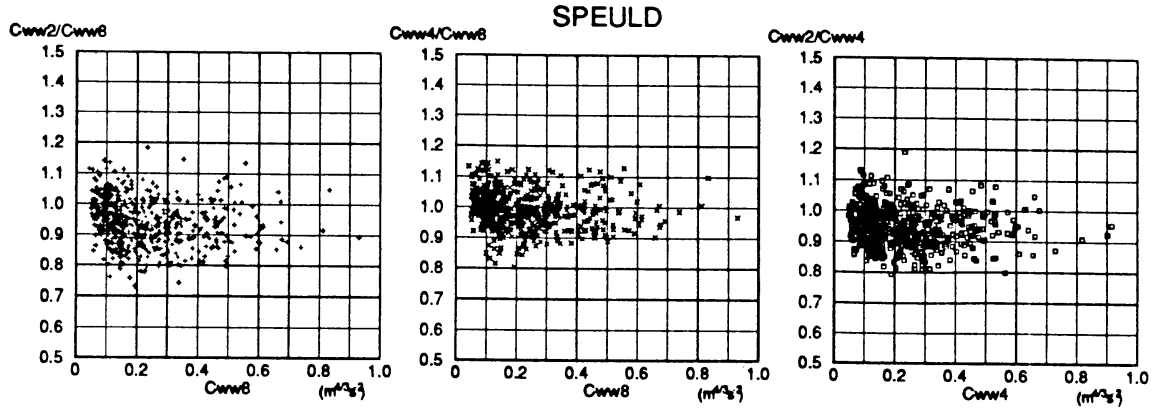

fig 5.8 Ratios of the structure parameter of vertical wind-velocity in Speuld.

In Cabauw (figure 5.9) the deviations from the averaged ratio become much greater than at the other two sites. Here they reach 25%. But also in Cabauw the lowest structure parameters were measured. As for Speuld the deviations grow for the very low structure parameter. This dataset also show the most outliers. Nevertheless the averaged values of Cww2/8 and Cww2/4 are good. Again Cww4/8 is too high, within 3%.

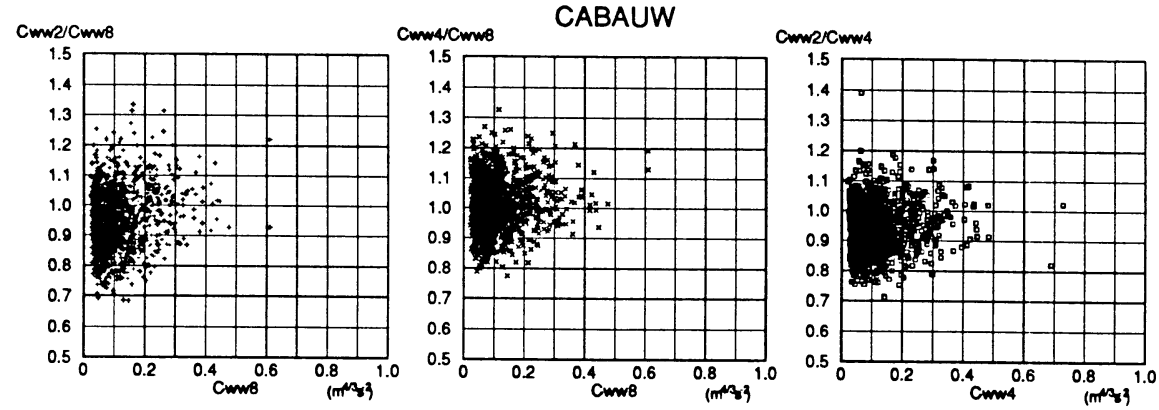

fig 5.9 Ratios of the structure parameter of vertical wind-velocity in Cabauw.

5.4 Scaling relations

At the end of the study of the structure parameter of vertical wind-velocity, some attention was paid to the scaling relations.

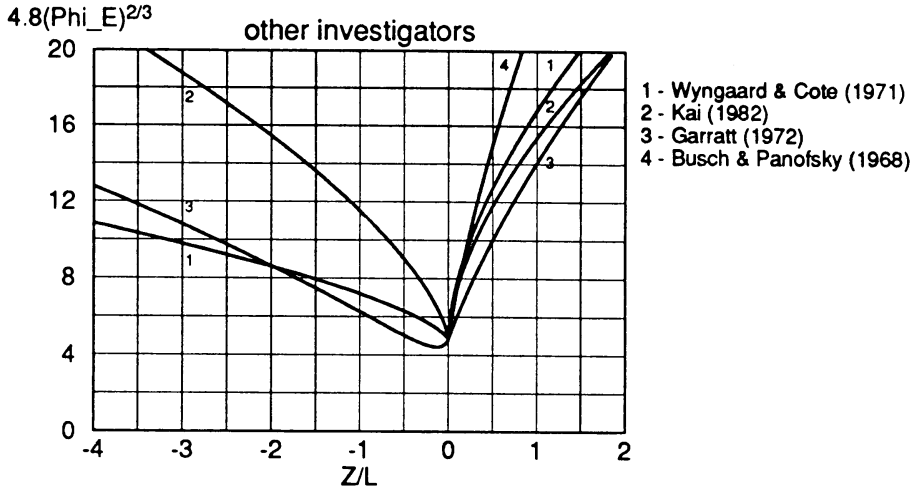

fig 5.10 Computed scaling relation for C_w^2 from dissipation relations.

Investigator	dissipaton relation	stability condition	structure pararameter relation
Wyngaard & Coté (1971)	$\Phi_\varepsilon(\frac{z}{L}) = (1+0.5\lvert\frac{z}{L}\rvert^{2/3})^{3/2}$	z/L < 0	$f_w(\frac{z}{L}) = 4.8(1+0.5\lvert\frac{z}{L}\rvert^{2/3})$
	$\Phi_\varepsilon(\frac{z}{L}) = (1+2.5(\frac{z}{L})^{3/5})^{3/2}$	z/L > 0	$f_w(\frac{z}{L}) = 4.8(1+2.5(\frac{z}{L})^{3/5})$
Kai (1982)	$\Phi_\varepsilon(\frac{z}{L}) = (1+1.4\lvert\frac{z}{L}\rvert^{2/3})^{3/2}$	z/L < 0	$f_w(\frac{z}{L}) = 4.8(1+1.4\lvert\frac{z}{L}\rvert^{2/3})$
	$\Phi_\varepsilon(\frac{z}{L}) = (1+2.2(\frac{z}{L})^{3/5})^{3/2}$	z/L > 0	$f_w(\frac{z}{L}) = 4.8(1+2.2(\frac{z}{L})^{3/5})$
Garratt (1972)	$\Phi_\varepsilon(\frac{z}{L}) = (1-16\frac{z}{L})^{-1/4} - \frac{z}{L}$	z/L < 0	$f_w(\frac{z}{L}) = 4.8[(1-16\frac{z}{L})^{-1/4} - \frac{z}{L}]^{2/3}$
	$\Phi_\varepsilon(\frac{z}{L}) = 1+4\frac{z}{L}$	z/L > 0	$f_w(\frac{z}{L}) = 4.8(1+4\frac{z}{L})^{2/3}$
Busch & Panofsky (1968)	$\Phi_\varepsilon(\frac{z}{L}) = 1+9\frac{z}{L}$	z/L > 0	$f_w(\frac{z}{L}) = 4.8(1+9\frac{z}{L})^{2/3}$

table 5.4 Scaling relations for the dissipation obtained by different investigators, and computed structure parameter scaling relations

In chapter 2 the relation between f_w and ϕ_ε was given. (2.21). Several investigators determined ϕ_ε in the atmospheric boundary layer. We plotted the computed scaling relations for C_w^2 in fig 5.10. What we obtained from the structure parameter measurements is put in the figures 5.11, 5.12 and 5.13. We compare these figures to obtain the common features.

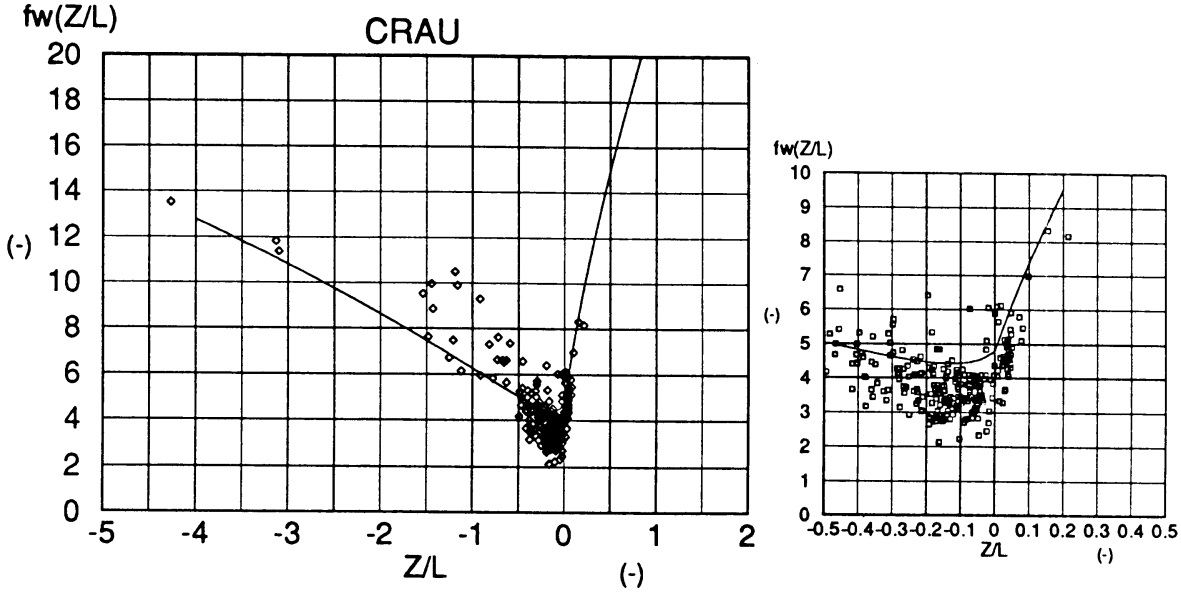

fig 5.11 Plot with the measured and scaled C_w^2 in Crau, against stabilit, and the best fitted curves from figure 5.10.

It is remarkable that the lowest point of the scaled structure parameters is not at z/L=0! This is in agreement with the results of Garratt(1972) who stated for the unstable side that $\Phi_\varepsilon=\Phi_m$- z/L. The other curves in fig 5.10 have their lowest point at z/L=0. The values of f_w at z/L=0 are somewhat low compared with the expected 4.8:

Crau : 4.0 ± 0.5

Speuld : 4.2 ± 0.5

Cabauw : 4.3 ± 0.7

The scatter in Cabauw is striking. At the unstable side we can discover three different tendencies.

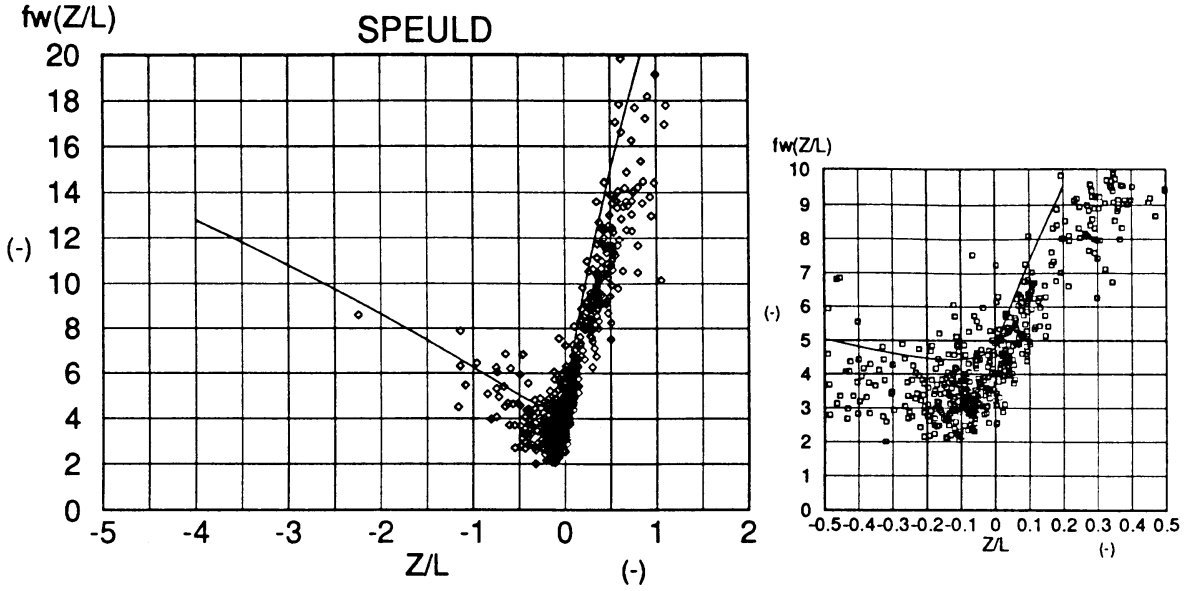

fig 5.12 Plot with the measured and scaled C_w^2 in Speuld, against stability, and the best fitted curves from figure 5.10.

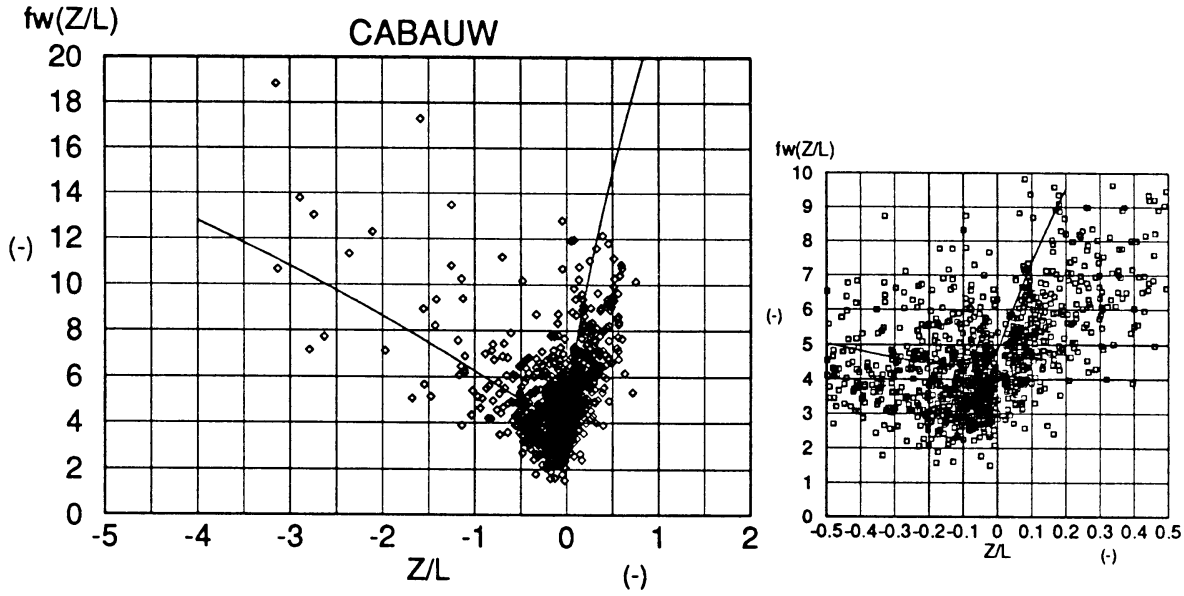

fig 5.13 Plot with the measured and scaled C_w^2 in Cabauw, against stability, and the best fitted curve from figure 5.10.

Comparing the result with the curves in fig 5.10 shows that at the stable side the function derived from the dissipation relation of Busch and Panofsky is a good fit for our data. Under unstable conditions Garratt's relation is a good approximation of our data. The curves of these relations are also plotted in the figures above.

6 DISCUSSION, CONCLUSIONS

6.1 The limits of the inertial subrange and isotropy

Ratios of structure parameters, measured over a different interval were used to test whether we measure in the inertial subrange or not, for a single velocity component. In §2.1 we argued this might also be a test for isotropy. The structure parameter ratio test produces results which are comparible with the spectral ratio test for isotropy.

If we compare figure 5.1 with the other figures in §5.1 we must realize that the frequency f is not the same as $1/2\Delta t$. If we measure a structure parameter over an interval Δt, we get most information about eddies with frequency $1/2\Delta t$, but smaller and bigger eddies do have some influence in that structure parameter.

Concerning the averaged values of C_w^2 in figure 5.4 it has to be marked that some points are averaged values over 200 measurements, on the other hand, two points are supported by only 10 values. More measurements could have produced a somewhat changed picture. Maybe better, maybe worse.

We conclude that the ratio of two different C_w^2's is a good and sensitive indicator of the inertial subrange limits in one component. There is reason to qualify it also as a test for isotropy. Further we conclude that the limits are reached earlier under stable conditions (at z/D=6) than in the unstable boundary layer (at z/D=3).

Further investigation can be directed towards the stability dependence of the increase of the ratios. Also can be investigated further if this test is a good test for isotropy and how the mechanism of 'becoming isotropic' works.

6.2 The structure parameter correction

Turbulence- and signal-theory was used to deduce a correction for the structurre parameter of vertical wind-velocity, measured with a sonic anemometer Kaijo Denki DAT-300. We can conclude that with this correction we can obtain well measured C_w^2's. A note of caution has to be included, because we did not have the exact impuls-response function. All information from Kaijo Denki was used to construct an ideal h(t) and three variations. The only realistic function did not change very much, so we used the ideal h1(t) for the correction. The realistic function h4(t) produces no N_{corr} factors other than zero. This fact support the reliability of the correction.

In Crau, a C_w^2 is measured over a time-interval of 0.04 seconds (Cww1). This means that $1/\Delta t = 25$ Hz. This frequency is higher than the sampling frequency of the SONIC. (20 Hz) Therefore it is not surprising that Cww1 cannot be corrected well enough. After correction its values are still too low.

Cabauw delivers a picture in which the ratio deviate more from the averaged value as for Crau and Speuld. The cause of the difference in scatter might be in the datalogger which is used in Cabauw, and not in Crau or Speuld. This instrument has a fixed sample period for measurements. Therefore it can happen that in one half hour averaged value the sampling program takes measurements of the SONIC only in the first part of the measurement cycle. Thus the assumption $k(\tau)=1, 0 \leq \tau < 1$ is not true for all measurements. This can cause sometimes high, sometimes too low measurements. This means more scatter! It is advisable to study whether the combination SONIC-Datalogger is a good one or not. Further it is recommendable to derive a correction for σ_w^2. The correction equations for C_w^2 suggest also a correction for σ_w^2.

6.3 The scaling relations

Attention was paid to scaling relations for C_w^2, to decide whether this structure parameter is good enough to be used for further analyses. Computed scaling relations from estimated relations for the dissipation are compatible with our results. Cabauw produces

too much scatter.

We didn't see a discontinuity at z/L=0 for the three datasets! At the unstable side Garratt seems to fit well, in stable conditions we choose Busch and Panofsky. There is not much difference between the three datasets! The lowest point of the scaled data is somewhat lower than expected.

We conclude that much has to be done in further analyzing these and other relations. A check of the Turbulent Kinetic Energy budget might be possible. Analyzing the precise influence of different terrain types also. The structure parameter of vertical wind-velocity appears to be a tractable quantity for use in analyses.

A1 Correction for U and u* measured by a sonic anemometer

Two corrections have to be executed for U, and also two for u_*. One of these has to be applied for both quantities: the correction for the angle between the SONIC orientation and the mean wind direction. So we are dealing with three different corrections for these quantities. The correction for the angle-difference is deduced and tested by Bosveld (1995). We only give the correction equations for U and u*:

$$U = \frac{U^m}{(1-0.08\varphi^2)}$$
$$u_* = \frac{u_*^m}{\sqrt{(1-0.08\varphi^2)}} \qquad \text{(A1.1)}$$

U^m and u_*^m are the measured values of U and u_*. The difference-angle is φ, in radials. The application of this correction is restricted to a fixed interval for φ: $-1.047 < \varphi < 1.047$ (-60, +60 degrees)

The friction velocity (u_*)has also to be corrected for tilting. This correction is described by Duyzer and Bosveld (1989). They obtained for the same type of SONIC and sensor:

$$\langle u'w'\rangle^m = \langle u'w'\rangle + 0.024\langle u'u'\rangle \qquad \text{(A1.2)}$$

Thus for u_*:

$$u_* = \sqrt{-(\langle u'w'\rangle^m - 0.024\langle u'u'\rangle)} \qquad \text{(A1.3)}$$

The accents denote the fluctuating part of the velocity component. We corrected u_* first for tilting and subsequently for the difference in angle.

The last correction is for the length of the wind-vector. Using a SONIC usually $\bar{u}_{sn}$ is defined as the length of the averaged wind-vector:

$$\overline{u}_{sn} = \sqrt{\overline{u}^2_{son} + \overline{v}^2_{son}} \qquad \text{(A1.4)}$$

Where u_{son} and v_{son} are the components measured by the SONIC. The bar over u_{sn}, u_{son} and v_{son} stands for time-averaging. For the calculation of the structure parameters we need the advection velocity of the smaller eddies along the sensor:

$$U = \overline{\sqrt{u^2 + v^2}} \qquad \text{(A1.5)}$$

Here u and v are the longitudinal and lateral windcomponents relative to the average wind vector. U is the averaged length of the wind-vector. It can be verified that the v-component always lengthens the wind-vector. Therefore the averaged length of the wind-vector is bigger than only the averaged u-component.

We rewrite (A1.5):

$$U = \overline{u}\overline{\sqrt{1+2\frac{u'}{\overline{u}} + \frac{u'^2 + v'^2}{\overline{u}^2}}} \qquad \text{(A1.6)}$$

The square root term can be developed, we neglect terms of third order and higher and derive for U:

$$U = \overline{\overline{u}\left(1+\frac{u'}{\overline{u}} + \frac{1}{2}\frac{v'^2}{\overline{u}^2}\right)} \qquad \text{(A1.7)}$$

Of course $\overline{u'}$ is zero, so we erase that term and we are left with:

$$U = \overline{u} + \frac{1}{2}\frac{\overline{v'^2}}{\overline{u}} \qquad \text{(A1.8)}$$

This is the correction we applied to $\overline{u}$, in the datasets called FFSN. Especially for low windspeed this correction is important. Also for the structure parameter correction which at low windspeeds changes a lot in the correction factors.

A2 Sonic specifications

4. SPECIFICATIONS

MODEL DA(T)-310 —— Probe TR-61A ——

ITEM			
Measuring Method			Time-sharing transmission/reception switchover type ultrasonic pulse emission.
Measuring Range			A, B, W axis 0 ~ ± 30 m/s
			Temperature* T : -10 ~ +40°C Fluctuation Temp.* T′: T_0 ~ ± 5°C (T_0 : Central Temperature)
Resolution			Wind speed 0.005 m/s Temperture* 0.025 °C
Accuracy			within ± 1 %
Number of Measurement Repetitions			approx. 20 /sec
Response			10 Hz
Coordinates Conversion	Input		Wind Speed Conponents A, B
	Operational Equation		$X = \frac{1}{\sqrt{3}}(A-B)$ $Y = A + B$
	Accuracy		within ± 1 %
Wind Speed Components Output	OUT 1		A, B, W 0 ~ ± 10 m/s / 0 ~ ± 1V (Max. 8V)
	OUT 2		0 ~ ± F·S / 0 ~ ± 1V (Max. 10V)
		F·S	A, B : ± 5, ± 10, ± 25, ± 50 m/s
			W : ± 1, ± 2, ± 5, ± 10 m/s
Vector Synthesizer Circuit	Input		X, Y Wind Speed Conponents
	Operational Equation	U	$U = \sqrt{X^2+Y^2}$
		θ	$\theta = \tan^{-1}(X/Y)$
	Accuracy	U	within ± 1 % (for F-S)
		θ	within ± 5°
	Output	U ($\bar{U}$)	0 ~ F·S / 0 ~ 1V , F·S : 5, 10, 25, 50 m/s
		θ ($\bar{\theta}$)	0 ~ 540° / 0 ~ 1V
Thermometer* Output	OUT 1		T -10 ~ +40°C / -0.2 ~ 0.8V
	OUT 2		T′ T_0 ~ ± 5°C / 0 ~ ± 1V
Output Impedance			Max. 1Ω or below (Max. 5mA)
Output Indicator			DC Voltmeter, Class 2.5 (±1V and 1V)
Output Connector			Front Panel: BNC connector, OUT1 and OUT2 (for X, Y, W, T), U($\bar{U}$), θ($\bar{\theta}$) Rear Panel : RM21TR-15S, OUT1 (for X, Y, W, T), U($\bar{U}$), θ($\bar{\theta}$)
Caliblation Signal			-1V, 0V, +1V : OUT2, U, θ
Probe / Junction Box			TR-61A (Span 20cm) / QA-60A
Operating Temperature Range			Main Unit : 0 ~ 40°C / Probe, Junction Box : -10 ~ 50°C
Operating Humidity Range			40 ~ 85 %
Power Supply			AC 100/115/220V ± 10%, 50/60Hz

* DAT-310 only.

(NOTE) If a surface of Probe Head is covered with ice, It is not able to measure wind speed and temperature.

A3 Dataset description files

COLOMN DISCRIPTION OF DATA-BASE CRAU

0	DAG	-	0	TYDIDENTIFIKATIE
1	BTYD	min	0	-
2	ETYD	-	0	-
3	-	-	0	-
4	U	m/s	0	Lengte WindVector Sonic, gecorrigeerd voor aanstr.hoek
5	NSAMP	-	0	AANTAL SAMPELS
6	FFSN	m/s	3	WINDSNELHEID SONIC
7	DDSN	o	1	WINDRICHTING SONIC
8	U*	m/s	4	WRIJVINGSSNELHEID EDDY-METHODE
9	DQDV	g/Kg/V	3	HELLING IJKKROMME LYAL IN WERKPUNT
10	VOLN	V	3	IJKKROMME VERSCHUIVING LYAL
11	QLAAG	g/Kg	3	SPECIFIEKE VOCHTIGHEID LAGE SENSOR
12	DELQ	g/Kg	4	SPECIFIEKE VOCHTIGHEID LAGE-HOGE SENSOR
13	BWED	0	2	BOWENVERHOUDING EDDY-METHODE
14	HEDDY	W/m2	1	SENSIBELE WARMTEFLUX EDDY-METHODE
15	LEEDDY	W/m2	1	LATENTE WARMTEFLUX EDDY-METHODE
16	H+LE	W/m2	1	TOTALE WARMTEFLUX EDDY-METHODE
17	LOED	m	0	OBHOEKOV LENGTE EDDY-METHODE
18	BWST	0	2	BOWENVERHOUDING STRUCTUUR PARAMETERS
19	BWPR	0	2	BOWENVERHOUDING PROFIEL-METHODE
20	QHUT	g/Kg	3	SPECIFIEKE VOCHTIGHEID HUT
21	TDAUW	oC	2	DAUWPUNTS TEMPERATUUR HUT
22	THEIM	oC	2	STRALINGS TEMPERATUUR HEIMANN
23	NRAIN	0	2	FRACTIE VAN DE SAMPELS WAARIN REGENMELDER NAT MELDT
24	ROTB	o	1	BEGINSTAND ROTOR
25	ROTE	o	1	EINDSTAND ROTOR
26	HPR	W/m2	1	SENSIBELE WARMTEFLUX PROFIEL-METHODE
27	LEPR	W/m2	1	LATENTE WARMTEFLUX PROFIEL-METHODE
28	HLEPR	W/m2	1	TOTALE WARMTE FLUX PROFIEL-METHODE
29	U*PR	m/s	4	WRIJVINGS SNELHEID PROFIEL-METHODE
30	LOPR	m	0	OBHUKOV LENGTE PROFIEL-METHODE
31	-	-	0	-
32	KLOK	V	2	KLOK SIGNAAL
33	-		0	
34	RAIN	V	2	REGEN MELDER
35	ROTR	o	1	ROTOR SIGNAAL
36	USON	m/s	3	WIND LONGITUDINAAL SONIC
37	VSON	m/s	3	WIND LATERAAL SONIC
38	WSON	m/s	4	WIND VERTIKAAL SONIC
39	TSON	K	2	SONISCHE TEMPERATUUR (DWARSWIND GEKORRIGEERD)
40	TPTA	K	3	TEMPERATUUR PT-ELEMENT
41	LYAL	V	3	LYAL VOLTAGE
42	TLAAG	oC	2	TEMPERATUUR LAGE SENSOR
43	TDD	K	3	DROOG-DROOG VERSCHIL HOGE- EN LAGE SENSOR
44	TNN	K	3	NAT-NAT VERSCHIL HOGE- EN LAGE SENSOR
45	TDNH	K	3	DROOG-NAT VERSCHIL HOGE SENSOR
46	ULAAG	m/s	3	WINDSNELHEID LAGE CUP-ANEMOMETER
47	UMIDD	m/s	3	WINDSNELHEID MIDDELSTE CUP-ANEMOMETER
48	UHOOG	m/s	3	WINDSNELHEID HOGE CUP-ANEMOMETER
49	THUT	oC	2	TEMPERATUUR HUT
50	RHUT	%	1	RELATIEVE VOCHTIGHEID HUT
51	FF10	m/s	3	WIND 10 METER
52	DD10	o	1	WINDRICHTING 10 METER
53	QNET	W/m2	1	NETTO STRALING
54	GLOB	W/m2	1	GLOBALE STRALING
55	HEIM	V	3	HEIMANN INFRAROOD SIGNAAL

56	-	-	0	-
57	U*COR	m/s	0	Wrijvingsnelheid gecor voor opstroming en aanstr.hoek
58	LOBH	m	0	ObhukovLengte met gecor U*
59	-	-	0	-
60	SKLOK	V	2	SDV. KLOK SIGNAAL
61	-	-	0	-
62	SRAIN	V	2	SDV. REGENMELDER
63	SROTR	o	1	SDV. ROTOR SIGNAAL
64	SUSON	m/s	3	SDV. LONGITUDINALE WIND SONIC
65	SVSON	m/s	3	SDV. LATERALE WIND SONIC
66	SWSON	m/s	3	SDV. VERTIKALE WIND SONIC
67	STSON	K	3	SDV. SONISCHE TEMPERATUUR (DWARSWIND GEKORRIGEERD)
68	STPTA	K	3	SDV. TEMPERATUUR PT-ELEMENT
69	SLYAL	V	4	SDV. LYAL VOLTAGE
70	STLAAG	K	3	SDV. TEMPERATUUR LAGE SENSOR
71	STDD	K	3	SDV. DROOG-DROOG VERSCHIL HOGE- EN LAGE SENSOR
72	STNN	K	3	SDV. NAT-NAT VERSCHIL HOGE- EN LAGE SENSOR
73	STDNH	K	3	SDV. DROOG-NAT VERSCHIL HOGE SENSOR
74	SULAAG	m/s	3	SDV. WINDSNELHEID LAGE CUP-ANEMOMETER
75	SUMIDD	m/s	3	SDV. WINDSNELHEID MIDDELSTE CUP-ANEMOMETER
76	SUHOOG	m/s	3	SDV. WINDSNELHEID HOGE CUP-ANEMOMETER
77	STHUT	K	3	SDV. TEMPERATUUR HUT
78	SRHUT	%	3	SDV. RELATIEVE VOCHTIGHEID HUT
79	SFF10	m/s	3	SDV. WINDSNELHEID 10 METER
80	SDD10	o	1	SDV. WINDRICHTING 10 METER
81	SQNET	W/m2	1	SDV. NETTO STRALING
82	SGLOB	W/m2	1	SDV. GLOBALE STRALING
83	SHEIM	V	3	SDV. HEIMANN INFRAROOD SIGNAAL
84	<UU>	(m/s)2	3	VARIANTIE LONGITUDINALE WIND
85	<UV>	(m/s)2	3	KORRELATIE LONGITUDINALE- EN LATERALE WIND
86	<UW>	(m/s)2	4	STRESS
87	<US>	km/s	4	KORRELATIE LONGITUDINALE WIND EN TEMPERATUUR SONIC
88	<UT>	Km/s	4	KORRELATIE LONGITUDINALE WIND EN TEMPERATUUR PT
89	<UQ>	gm/Kgs	4	KORRELATIE LONGITUDINALE WIND EN SPECIFIEKE VOCHTIGHEID
90	<VV>	(m/s)2	3	VARIANTIE LATERALE WIND
91	<VW>	(m/s)2	4	LATERALE STRESS
92	<VS>	km/s	4	KORRELATIE LATERALE WIND EN TEMPERATUUR SONIC
93	<VT>	Km/s	4	KORRELATIE LATERALE WIND EN TEMPERATUUR PT
94	<VQ>	gm/Kgs	4	KORRELATIE LATERALE WIND EN SPECIFIEKE VOCHTIGHEID
95	<WW>	(m/s)2	4	VARIANTIE VERTIKALE WIND
96	<WS>	km/s	4	TEMPERATUUR FLUX SONIC
97	<WT>	Km/s	4	TEMPERATUUR FLUX PT
98	<WQ>	gm/Kgs	4	SPECIFIEKE VOCHTIGHEIDS FLUX
99	<SS>	K2	4	VARIANTIE TEMPERATUUR SONIC
100	<ST>	K2	4	KORRELATIE TEMPERATUREN SONIC EN PT
101	<SQ>	gK/Kg	4	KORRELATIE SPECIFIEKE VOCHTIGHEID EN TEMPERATUUR SONIC
102	<TT>	K2	4	VARIANTIE TEMPERATUUR PT
103	<QT>	gK/Kg	4	KORRELATIE SPECIFIEKE VOCHTIGHEID EN TEMPERATUUR PT
104	<QQ>	g2/Kg2	5	VARIANTIE SPECIFIEKE VOCHTIGHEID
105	-	-	0	-
106	-	-	0	-
107	-	-	0	-
108	-	-	0	-
109	-	-	0	-
110	-	-	0	-
111	-	-	0	-
112	CUU1	*	4	STRUCTUUR PARAMETER LONGITUDINALE WIND .04 SEC
113	CUU2	*	4	STRUCTUUR PARAMETER LONGITUDINALE WIND .08 SEC
114	CUU4	*	4	STRUCTUUR PARAMETER LONGITUDINALE WIND .16 SEC
115	CVV1	*	4	STRUCTUUR PARAMETER LATERALE WIND .04 SEC

116	CVV2	*	4	STRUCTUUR PARAMETER LATERALE WIND .08 SEC
117	CVV4	*	4	STRUCTUUR PARAMETER LATERALE WIND .16 SEC
118	CWW1	*	4	STRUCTUUR PARAMETER VERTIKALE WIND .04 SEC
119	CWW2	*	4	STRUCTUUR PARAMETER VERTIKALE WIND .08 SEC
120	CWW4	*	4	STRUCTUUR PARAMETER VERTIKALE WIND .16 SEC
121	CSS1	*	4	STRUCTUUR PARAMETER SONISCHE-TEMPERATUUR .04 SEC
122	CSS2	*	4	STRUCTUUR PARAMETER SONISCHE-TEMPERATUUR .08 SEC
123	CSS4	*	4	STRUCTUUR PARAMETER SONISCHE-TEMPERATUUR .16 SEC
124	CTT1	*	4	STRUCTUUR PARAMETER PT-TEMPERATUUR .04 SEC
125	CTT2	*	4	STRUCTUUR PARAMETER PT-TEMPERATUUR .08 SEC
126	CTT4	*	4	STRUCTUUR PARAMETER PT-TEMPERATUUR .16 SEC
127	CQQ1	*	4	STRUCTUUR PARAMETER VOCHT .04 SEC
128	CQQ2	*	4	STRUCTUUR PARAMETER VOCHT .08 SEC
129	CQQ4	*	4	STRUCTUUR PARAMETER VOCHT .16 SEC
130	CUV1	*	4	STRUCTUUR PARAMETER LONGT.-LATERALE WIND .04 SEC
131	CUV2	*	4	STRUCTUUR PARAMETER LONGT.-LATERALE WIND .08 SEC
132	CUV4	*	4	STRUCTUUR PARAMETER LONGT.-LATERALE WIND .16 SEC
133	CTQ1	*	4	STRUCTUUR PARAMETER TEMP.PT EN VOCHT .04 SEC
134	CTQ2	*	4	STRUCTUUR PARAMETER TEMP.PT EN VOCHT .08 SEC
135	CTQ4	*	4	STRUCTUUR PARAMETER TEMP.PT EN VOCHT .16 SEC
136	-	-	0	-
137	CTT	*	4	TEMPERATUUR STRUKTUUR-PARAMETER (GEMIDDELD)
138	CTQ	*	4	TEMP.-VOCHT STRUKTUUR-PARAMETER (GEMIDDELD)
139	CQQ	*	4	VOCHT STRUKTUUR-PARAMETER (GEMIDDELD)
140	-	-	0	-
141	-	-	0	-
142	-	-	0	-
143	-	-	0	-
144	-	-	0	-
145	-	-	0	-
146	-	-	0	-
147	-	-	0	-
148	-	-	0	-
149	-	-	0	-
150	-	-	0	-
151	-	-	0	-
152	-	-	0	-
153	-	-	0	-
154	-	-	0	-
155	-	-	0	-
156	-	-	0	-
157	-	-	0	-
158	-	-	0	-
159	-	-	0	-
160	-	-	0	-
161	-	-	0	-
162	-	-	0	-
163	-	-	0	-
164	-	-	0	-
165	-	-	0	-
166	-	-	0	-
167	-	-	0	-
168	-	-	0	-
169	-	-	0	-
170	-	-	0	-
171	-	-	0	-
172	-	-	0	-
173	-	-	0	-
174	-	-	0	-
175	-	-	0	-

176	-	-	0	-
177	-	-	0	-
178	-	-	0	-
179	-	-	0	-
180	-	-	0	-
181	-	-	0	-
182	-	-	0	-
183	-	-	0	-
184	-	-	0	-
185	-	-	0	-
186	-	-	0	-
187	-	-	0	-
188	-	-	0	-
189	-	-	0	-
190	-	-	0	-
191	-	-	0	-
192	NULV	m	2	NULVLAK VERPLAATSING
193	ZFF	m	2	MEETHOOGTE STANDAARD WINDMETING
194	ZSONIC	m	2	MEETHOOGTE SONICHE ANEMOMETER
195	ZUH	m	2	MEETHOOGTE WINDPROFIEL HOOG
196	ZUM	m	2	MEETHOOGTE WINDPROFIEL MIDDEN
197	ZUL	m	2	MEETHOOGTE WINDPROFIEL LAAG
198	ZTH	m	2	MEETHOOGTE TEMPERATUUR PROFIEL HOOG
199	ZTL	m	2	MEETHOOGTE TEMPERATUUR PROFIEL LAAG

COLOMN DISCRIPTION OF DATA-BASE SPEULD

0	DAG	-	B0	TYDIDENTIFIKATIE
1	BTYD	min	B0	BEGIN TIJD
2	ETYD	-	B0	EIND TIJD
3	DAGNR	-	0	DAGNUMMER V.A. 1/1+FRACTIE VAN DE DAG
4	DLOTNR	-	0	DAGNUMMER V.A. 1900 + FRACTIE VAN DE DAG
5	NSAMP	-	B0	AANTAL SAMPELS
6	FFSN	m/s	B3	WINDSNELHEID SONIC
7	DDSN	o	B1	WINDRICHTING SONIC
8	U*	m/s	A4	WRIJVINGSSNELHEID EDDY-METHODE
9	DQDV	g/Kg/V	B3	HELLING IJKKROMME LYAL IN WERKPUNT
10	VOLN	V	B3	IJKKROMME VERSCHUIVING LYAL
11	TO	K	A2	TEMPERATUUR NIVO 0
12	QO	g/Kg	A3	SPECIFIEKE VOCHTIGHEID NIVO 0
13	T1	K	A2	TEMPERATUUR NIVO 1
14	Q1	g/Kg	A3	SPECIFIEKE VOCHTIGHEID NIVO 1
15	Q21	g/Kg	A4	SPECIFIEKE VOCHTIGHEIDS VERSCHIL NIVO 2-1
16	Q32	g/Kg	A4	SPECIFIEKE VOCHTIGHEIDS VERSCHIL NIVO 3-2
17	Q43	g/Kg	A4	SPECIFIEKE VOCHTIGHEIDS VERSCHIL NIVO 4-3
18	DELT	K	A3	ROND REKENEN TEMPERATUUR PROFIELEN
19	THEIM	oC	A2	INFRAROOD STRALINGS TEMPERATUUR KRONEN DAK
20	LOBH	m	A0	OBHUKOV LENGTE
21	H+LE	W/m2	A1	TOTALE TURBULENTE WARMTE FLUX
22	BWED	0	A2	BOWEN VERHOUDING EDDY-CORRELATIE
23	BWPR	0	A2	BOWEN VERHOUDING PROFIELEN
24	TPOT21	K	A3	POTENTIEEL TEMPERATUUR VERSCHIL NIVO 2-1
25	TPOT32	K	A3	POTENTIEEL TEMPERATUUR VERSCHIL NIVO 3-2
26	TPOT43	K	A3	POTENTIEEL TEMPERATUUR VERSCHIL NIVO 4-3
27	HEDDY	W/m2	A1	SENSIBELE TURBULENTE WARMTE STROOM
28	LEEDDY	W/m2	A1	LATENTE TURBULENTE WARMTE STROOM
29	TDEWO	oC	A2	DAUWPUNT NIVO 0
30	TDEW1	oC	A2	DAUWPUNT NIVO 1
31	NRAIN	0	B2	FRACTIE NATTE SAMPELS
32	ROTRB	o	B1	ROTOR BEGIN STAND
33	ROTRE	o	B1	ROTOR EIND STAND
34	ROTR	o	B1	ROTOR SIGNAAL
35	USON	m/s	B3	WIND LONGITUDINAAL SONIC
36	VSON	m/s	B3	WIND LATERAAL SONIC
37	WSON	m/s	B4	WIND VERTIKAAL SONIC
38	TSON	K	B2	SONISCHE TEMPERATUUR
39	TPTA	K	B3	TEMPERATUUR PT-ELEMENT
40	LYAL	V	B3	LYAL VOLTAGE
41	TBL1	oC	B2	TEMPERATUUR PT-500 NIVO 1
42	TD1B	K	B3	TEMPERATUUR VERSCHIL NIVO1-PT500(1)
43	TD21	K	B3	TEMPERATUUR VERSCHIL DROOG NIVO 2-1
44	TD32	K	B3	TEMPERATUUR VERSCHIL DROOG NIVO 3-2
45	TD43	K	B3	TEMPERATUUR VERSCHIL DROOG NIVO 4-3
46	TDN4	K	B3	TEMPERATUUR VERSCHIL DROOG-NAT NIVO 4
47	TN43	K	B3	TEMPERATUUR VERSCHIL NAT NIVO 4-3
48	TN32	K	B3	TEMPERATUUR VERSCHIL NAT NIVO 3-2
49	TN21	K	B3	TEMPERATUUR VERSCHIL NAT NIVO 2-1
50	TN1B	K	B3	TEMPERATUUR VERSCHIL NAT NIVO1-PT500(1)
51	TBLO	oC	B2	TEMPERATUUR PT500 NIVO 0
52	TDOB	K	B3	TEMPERATUUR VERSCHIL DROOG NIVOO-PT500(O)
53	TNOB	K	B3	TEMPERATUUR VERSCHIL NAT NIVOO-PT500(O)
54	UCUPO	m/s	B3	WINDSNELHEID NIVO 0
55	UCUP1	m/s	B3	WINDSNELHEID NIVO 1
56	UCUP2	m/s	B3	WINDSNELHEID NIVO 2

57	UCUP3	m/s	B3	WINDSNELHEID NIVO 3
58	UCUP4	m/s	B3	WINDSNELHEID NIVO 4
59	DDVN4	o	B1	WINDRICHTING NIVO 4
60	GLOB	W/m2	B1	GLOBALE STRALING
61	QNET	W/m2	B1	NETTO STRALING
62	HEIM	V	B3	HEIMAN INFRAROOD STRALINGS METER
63	SCIN	V	B3	SCINTILLATIE METER
64	RAIN	V	B3	REGEN MELDER
65	YWAT	o	B3	Y-WATERPAS
66	XWAT	o	B3	X-WATERPAS
67	OFFS	mV	B3	OFFSET SPANNING KORT GESLOTEN MINC-KANAAL
68	SROTR	o	B1	SDV. ROTOR SIGNAAL
69	SUSON	m/s	B3	SDV. WIND LONGITUDINAAL SONIC
70	SVSON	m/s	B3	SDV. WIND LATERAAL SONIC
71	SWSON	m/s	B3	SDV. WIND VERTIKAAL SONIC
72	STSON	K	B3	SDV. SONISCHE TEMPERATUUR
73	STPTA	K	B3	SDV. TEMPERATUUR PT-ELEMENT
74	SLYAL	V	B4	SDV. LYAL VOLTAGE
75	STBL1	oC	B3	SDV. TEMPERATUUR PT-500 NIVO 1
76	STD1B	K	B3	SDV. TEMPERATUUR VERSCHIL NIVO1-PT500(1)
77	STD21	K	B3	SDV. TEMPERATUUR VERSCHIL DROOG NIVO 2-1
78	STD32	K	B3	SDV. TEMPERATUUR VERSCHIL DROOG NIVO 3-2
79	STD43	K	B3	SDV. TEMPERATUUR VERSCHIL DROOG NIVO 4-3
80	STDN4	K	B3	SDV. TEMPERATUUR VERSCHIL DROOG-NAT NIVO 4
81	STN43	K	B3	SDV. TEMPERATUUR VERSCHIL NAT NIVO 4-3
82	STN32	K	B3	SDV. TEMPERATUUR VERSCHIL NAT NIVO 3-2
83	STN21	K	B3	SDV. TEMPERATUUR VERSCHIL NAT NIVO 2-1
84	STN1B	K	B3	SDV. TEMPERATUUR VERSCHIL NAT NIVO1-PT500(1)
85	STBL0	oC	B3	SDV. TEMPERATUUR PT500 NIVO 0
86	STDOB	K	B3	SDV. TEMPERATUUR VERSCHIL DROOG NIVO0-PT500(0)
87	STNOB	K	B3	SDV. TEMPERATUUR VERSCHIL NAT NIVO0-PT500(0)
88	SUCUP0	m/s	B3	SDV. WINDSNELHEID NIVO 0
89	SUCUP1	m/s	B3	SDV. WINDSNELHEID NIVO 1
90	SUCUP2	m/s	B3	SDV. WINDSNELHEID NIVO 2
91	SUCUP3	m/s	B3	WINDSNELHEID NIVO 3
92	SUCUP4	m/s	B3	WINDSNELHEID NIVO 4
93	SDDVN4	o	B3	WINDRICHTING NIVO 4
94	SGLOB	W/m2	B1	GLOBALE STRALINGL
95	SQNET	W/m2	B1	NETTO STRALING
96	SHEIM	V	B3	HEIMAN INFRAROOD STRALINGS METER
97	SSCIN	V	B3	SCINTILLATIE METER
98	SRAIN	V	B3	REGEN MELDER
99	SYWAT	o	B3	Y-WATERPAS
100	SXWAT	o	B3	X-WATERPAS
101	SOFFS	mV	B3	OFFSET SPANNING KORT GESLOTEN MINC-KANAAL
102	<UU>	(m/s)2	B3	VARIANTIE LONGITUDINALE WIND
103	<UV>	(m/s)2	B3	KORRELATIE LONGITUDINALE- EN LATERALE WIND
104	<UW>	(m/s)2	B4	STRESS
105	<US>	Km/s	B4	KORRELATIE LONGITUDINALE WIND EN TEMPERATUUR SONIC
106	<UT>	Km/s	B4	KORRELATIE LONGITUDINALE WIND EN TEMPERATUUR PT
107	<UQ>	gm/Kgs	B4	KORRELATIE LONGITUDINALE WIND EN SPECIFIEKE VOCHTIGHEID
108	<VV>	(m/s)2	B3	VARIANTIE LATERALE WIND
109	<VW>	(m/s)2	B4	LATERALE STRESS
110	<VS>	km/s	B4	KORRELATIE LATERALE WIND EN TEMPERATUUR SONIC
111	<VT>	Km/s	B4	KORRELATIE LATERALE WIND EN TEMPERATUUR PT
112	<VQ>	gm/Kgs	B4	KORRELATIE LATERALE WIND EN SPECIFIEKE VOCHTIGHEID
113	<WW>	(m/s)2	B4	VARIANTIE VERTIKALE WIND
114	<WS>	km/s	B4	TEMPERATUUR FLUX SONIC
115	<WT>	Km/s	B4	TEMPERATUUR FLUX PT
116	<WQ>	gm/Kgs	B4	SPECIFIEKE VOCHTIGHEIDS FLUX

117	<SS>	K2	B4	VARIANTIE TEMPERATUUR SONIC
118	<ST>	K2	B4	KORRELATIE TEMPERATUREN SONIC EN PT
119	<SQ>	gK/Kg	B4	KORRELATIE SPECIFIEKE VOCHTIGHEID EN TEMPERATUUR SONIC
120	<TT>	K2	B4	VARIANTIE TEMPERATUUR PT
121	<QT>	gK/Kg	B4	KORRELATIE SPECIFIEKE VOCHTIGHEID EN TEMPERATUUR PT
122	<QQ>	g2/Kg2	B5	VARIANTIE SPECIFIEKE VOCHTIGHEID
123	CAA1	-	B4	-
124	CAA2	-	B4	-
125	CAA4	-	B4	-
126	CBB1	-	B4	-
127	CBB2	-	B4	-
128	CBB4	-	B4	-
129	CWW1	-	B4	-
130	CWW2	-	B4	-
131	CWW4	-	B4	-
132	CSS1	-	B4	-
133	CSS2	-	B4	-
134	CSS4	-	B4	-
135	CTT1	-	B4	-
136	CTT2	-	B4	-
137	CTT4	-	B4	-
138	CQQ1	-	B4	-
139	CQQ2	-	B4	STRUCTURE PARAMETER MOISTURE T=0.16 S
140	CQQ4	-	B4	STRUCTURE PARAMETER MOISTURE T=0.32 S
141	CAB1	-	B4	CROSS STRUCTURE PARAMETER HORIZONTAL WIND T=0.08 S
142	CAB2	-	B4	CROSS STRUCTURE PARAMETER HORIZONTAL WIND T=0.16 S
143	CAB4	-	B4	CROSS STRUCTURE PARAMETER HORIZONTAL WIND T=0.32 S
144	CTQ1	-	B4	CROSS STRUCTURE PARAMETER TEMP AND MOIST T=0.08 S
145	CTQ2	-	B4	CROSS STRUCTURE PARAMETER TEMP AND MOIST T=0.16 S
146	CTQ4	-	B4	CROSS STRUCTURE PARAMETER TEMP AND MOIST T=0.32 S
147	CUU1	-	B4	-
148	CUU2	-	B4	-
149	CUU4	-	B4	-
150	CVV1	-	B4	-
151	CVV2	-	B4	-
152	CVV4	-	B4	-
153	CUV1	-	B4	-
154	CUV2	-	B4	-
155	CUV4	-	B4	-
156	DELDDS	o	A0	-
157	USTCOR	m/s	A0	U* GECORR. VOOR OBSTRUCTIE+AANSTROOMHOEK
158	CNN	-	X0	BREKINGS INDEX STRUCTUUR PARAMETER
159	WB	Km/s	A4	ALLEEN WIND GECORR. SONIC-TEMP.FLUX, (BUYONCY FLUX)
160	QDEF	g/Kg	X4	SPECIFIC MOISTURE DEFICIT
161	T*	K	X3	TURBULENT TEMPERATURE SCALE
162	Q*	g/Kg	X3	TURBULENT HUMIDITY SCALE
163	KSI	0	A4	STABILITY PARAMETER (Z-D)/L
164	U	m/s	B3	Gecorrigeerde Wind-Vector Lengte
165	-	-	X0	-
166	GLOBCL	W/m2	A1	GLOBALE STRALING BIJ HELDERE LUCHT
167	UCUP43	m/s	A3	WINDSNELHEIDS VERSCHIL NIVO 4-3
168	UCUP32	m/s	A3	WINDSNELHEIDS VERSCHIL NIVO 4-2
169	UCUP21	m/s	A3	WINDSNELHEIDS VERSCHIL NIVO 4-1
170	HSON	W/m2	A1	SONISCHE WARMTEFLUX WIND GEKORRIGEERD
171	QNCORR	W/m2	A1	QNET GECORRIGEERD VOOR TILT
172	HPR	W/m2	A1	SENSIBELE WARMTEFLUX UIT PROFIEL NIVO 4-2
173	LEPR	W/m2	A1	LATENTE WARMTEFLUX UIT PROFIEL NIVO 4-2
174	LEBWSN	W/m2	A1	LATENTE WARMTEFLUX UIT HSON EN BWPR
175	USTPR	m/s	A3	WRIJVINGS SNELHEID UIT PROFIEL NIVO 4-2
176	FKSIPR	0	A4	STABILITEIT (Z-D)/L UIT PROFIEL NIVO 4-2

177	HBW	W/m2	A1	SENSIBELE WARMTE UIT QAIV EN BWPR
178	LEBW	W/m2	A1	LATENTE WARMTE UIT QAIV EN BWPR
179	GBIO	W/m2	A1	WARMTE FLUX NAAR DE BIOMASSA
180	GAIR	W/m2	A1	TOTALE WARMTE FLUX NAAR DE LUCHT Z<30M
181	QAIV	W/m2	A1	BESCHIKBARE WARMTE
182	LEMD	W/m2	A1	LATENTE WARMTE BIG-LEAF MODEL
183	LEBAL	W/m2	A1	LATENTE WARMTE UIT ENERGIE BALANS MET HSON
184	LEPOT	-	XO	-
185	P185	-	XO	-
186	-	-	XO	-
187	DELU	K	A3	RONDREKENEN TEMPERATUUR PROFIEL IN THERMO-SPANNING
188	ZNULVL	m	B2	NULVLAK VERPLAATSING
189	ZSONIC	m	B2	MEETHOOGTE SONISCHE ANEMOMETER
190	ZT4	m	B2	MEETHOOGTE TEMPERATUUR NIVO 4
191	ZT3	m	B2	MEETHOOGTE TEMPERATUUR NIVO 3
192	ZT2	m	B2	MEETHOOGTE TEMPERATUUR NIVO 2
193	ZT1	m	B2	MEETHOOGTE TEMPERATUUR NIVO 1
194	ZTO	m	B2	MEETHOOGTE TEMPERATUUR NIVO 0
195	ZU4	m	B2	MEETHOOGTE WIND NIVO 4
196	ZU3	m	B2	MEETHOOGTE WIND NIVO 3
197	ZU2	m	B2	MEETHOOGTE WIND NIVO 2
198	ZU1	m	B2	MEETHOOGTE WIND NIVO 1
199	ZUO	m	B2	MEETHOOGTE WIND NIVO 0

COLOMN DISCRIPTION OF DATA-BASE CABNACHT				
0	DAG	dag	0	-
1	BTYD	min	0	-
2	ETYD	min	0	-
3	-	-	0	-
4	FFSN	-	0	-
5	USON	m/s	0	-
6	VSON	m/s	0	-
7	WSON	m/s	0	-
8	TFM	K	0	-
9	TSON	oC	0	-
10	<UU>	m/s2	0	-
11	<VV>	m/s2	0	-
12	<WW>	m/s2	0	-
13	<TT>	K2	0	-
14	<SS>	K2	0	-
15	<UV>	m/s2	0	-
16	<UW>	m/s2	0	-
17	<UT>	Km/s	0	-
18	<US>	Km/s	0	-
19	<VW>	m/s2	0	-
20	<VT>	Km/s	0	-
21	<VS>	Km/s	0	-
22	<WT>	Km/s	0	-
23	<WS>	Km/s	0	-
24	<TS>	K2	0	-
25	TNTC	oC	0	-
26	ROTR	o	0	-
27	FF05	m/s	0	-
28	FF10	m/s	0	-
29	FF20	m/s	0	-
30	DD10	o	0	-
31	TD1	oC	0	-
32	TD21	K	0	-
33	TD32	K	0	-
34	TD43	K	0	-
35	RAIN	0	0	-
36	ROTE	o	0	-
37	CWW1	-	0	-
38	CWW2	-	0	-
39	CWW4	-	0	-
40	CTT1	-	0	-
41	CTT2	-	0	-
42	CTT4	-	0	-
43	NSAMP	0	0	-
44	LPHI	o	0	-
45	SH20	g/kg	0	-
46	SH10	g/kg	0	-
47	SH02	g/kg	0	-
48	SH06	g/kg	0	-
49	F200	m/s	0	-
50	QNET	W/m2	0	-
51	RM	mm	0	-
52	PP	mbar	0	-
53	zon	aanthu	0	-
54	WOL1	-	0	-
55	WOL2	-	0	-
56	WOL3	-	0	-

57	Uster	m/s	0	-
58	HPR	W/m2	0	-
59	HBOW	W/m2	0	-
60	LEPR	W/m2	0	-
61	LEBOW	W/m2	0	-
62	LEBAL	W/m2	0	-
63	Znul	m	0	-
64	DDSN	-	0	-
65	U	-	0	-
66	LOBH	l	0	-
67	-	-	0	-
68	-	-	0	-
69	-	-	0	-
70	-	-	0	-
71	-	-	0	-
72	-	-	0	-
73	-	-	0	-
74	-	-	0	-
75	-	-	0	-
76	-	-	0	-
77	-	-	0	-
78	-	-	0	-
79	-	-	0	-

B1Structure parameter correction programs

```
{
        Programma om de correcties te berekenen

        Date      : 06-06-91
        Programmer: Rik van der Ploeg
}
Program Correct;

Uses
   Crt,Dos;

Const
   Tr      = 0.0531;
   Tg      = Tr/6;
   D       = 0.20;
   u2_3    = -0.05;
   Ex      = 2/3-u2_3;
   SigmaW  = 1;
   Punten  = 10;
   MisVal  = -9999;

Var
   Parameter, B, N, Delta, I, Teller,Aantal,
   AantalFiles, FileNumber                    :Integer;
   P,G,R,Fl,FFSN,X,DeltaT,Tau,DeltaTau,
   Fc,Value                                   :Real;
   IData                                      :Array[1..5000,1..2] Of Real;
   IResp                                      :Array[0..20,0..3] of Real;
   Infile,Outfile                             :Text;
   Missing                                    :Boolean;
   Inputfile                                  :Array[1..10] Of String[8];

Function Macht(Arg,Eksponent :Real) : Real;

Begin
    If Arg <> 0 Then Macht := Exp(Eksponent*Ln(Arg))
    Else  Macht := 0;
End; {Macht}


Function Ilineint(Y,X :Real) : Real;

Var     R        : Real;

Begin
     Ilineint  := (X*X+0.75*Y*Y)*Macht(X*X+Y*Y,0.5*Ex-1)*(1-Y);
End;  { I }

Function IlineT(X : Real) : Real;

Var Coef2,Coef4,Coef6 : Real;

Begin
  Coef2   := (1-6*u2_3)/144;
  Coef4   := (1+3*u2_3)*(4+3*u2_3)/2160;
  Coef6   := (5+6*u2_3)*(4+3*u2_3)*(10+3*u2_3)/145152;
  IlineT   := Macht(X,Ex)*(0.5+Coef2*Macht(X,-2)+Coef4*Macht(X,-4)
                                                -Coef6*Macht(X,-6));
End;
```

```
Function IlineS (N1 : Integer; X :Real) : Real;

Var
    J                   : Integer;
    H, Y1, Y2, Y3,Sim   : Real;
Begin
    H   := 0.5/N1;          { Stapgrootte }
    Sim := 0;
    For J := 1 To N1 Do
    Begin
      Y1 :=(2*J-2)*H;
      Y2 :=Y1+H;
      Y3 :=Y2+H;
      Sim := Sim + Ilineint(Y1,X)+4*Ilineint(Y2,X)+Ilineint(Y3,X);
    End;
    IlineS := H*Sim/3;
End; {IlineS}

Function Iline(X :Real) : Real;

Var Fac                         : Real;
    Wijzer                      : Integer;

Begin

  If X > IData[Aantal,1] Then Iline := IlineT(X)
  Else
  Begin
    Fac    := 0.5;
    Wijzer := Round(Aantal*Fac);
    While Fac*Aantal > 1 Do
    Begin
       Fac := Fac/2;
       If X > IData[Wijzer,1] Then Wijzer := Wijzer + Round(Fac*Aantal)
       Else
         If X < IData[Wijzer,1] Then Wijzer := Wijzer - Round(Fac*Aantal)
       Else Fac := 0;
    End;
    If IData[Wijzer,1] > X Then Wijzer := Wijzer -1;
    Iline := IData[Wijzer,2]+(X-IData[Wijzer,1])/(IData[Wijzer+1,1]-
             IData[Wijzer,1])*(IData[Wijzer+1,2]-IData[Wijzer,2]);
  End;
End;

Function Ncorr(DTau :Real): Real;

Var I     : Integer;
    Nhulp : Real;

Begin
  Parameter:= Round(Ln(DTau*Tr/0.04)/Ln(2));
  Delta    := Round(DTau+0.5);
  Nhulp    := 0;
  For I := 1 To Delta+B Do
  Begin
    Nhulp := Nhulp + Iresp[I,Parameter];
  End;
  Ncorr := SigmaW *(Iresp[0,Parameter]+2*Nhulp) ;
End; { Ncorr }
```

```
Function Fcorr(DTau,P,G,R : Real): Real;

Var I     : Integer;
    Fhulp : Real;

Begin
  Parameter:= Round(Ln(DTau*Tr/0.04)/Ln(2));
  Delta    := Round(DTau+0.5);
  Fhulp    := (Iline(0)+Iline(G))*Iresp[0,Parameter];
  For I := 1 To Delta+B Do
  Begin
    Fhulp := Fhulp+(Iline(R*I-G)+2*Iline(R*I)+Iline(R*I+G))*Iresp[I,Parameter];
  End;
  Fcorr := -0.5/Macht(P,Ex)*Fhulp ;
End; { Fcorr }

Begin
    {   Open input en output, vraag gegevens
    }
    Teller := 0;
    Writeln('Inlezen Iresp data');
    Assign(Infile,'IRESP.OUT');
    Reset(Infile);
    Readln(Infile);
    Readln(Infile,B);
    Readln(Infile);
    Missing := False;
    I       := 0;
    While Not(Eof(Infile)) Do
    Begin
      For Parameter := 0 To 3 Do
      Begin
        Read(Infile,Iresp[I,Parameter]);
      End;
      Readln(Infile);
      I := I+1;
    End;
    Writeln('Inlezen Iline data!!');
    Assign(Infile,'ILINE.OUT');
    Reset(Infile);
    Readln(Infile); Readln(Infile);
    While Not(Eof(Infile)) Do
    Begin
      Teller := Teller +1;
      Readln(Infile,Idata[Teller,1],Idata[Teller,2]);
    End;
    Aantal := Teller;
    ClrScr;
    For Parameter := 0 To 3 Do
    Begin
      DeltaT  := Round(Macht(2,Parameter))*0.04;
      DeltaTau:= DeltaT/Tr;
      Writeln('Ncorr',Round(DeltaT/0.04),' :',Ncorr(DeltaTau):1:5);
    End;
    Writeln;
    Write('Inputfiles:?');
    AantalFiles := 0;
    Repeat
      GotoXY(12,WhereY);
```

```
      AantalFiles := AantalFiles+1;
      Readln(inputfile[AantalFiles]);
    Until inputfile[AantalFiles] = '';
    Writeln;
    AantalFiles := AantalFiles-1;
    For FileNumber := 1 To AantalFiles Do
    Begin
       Writeln('File: ',inputfile[FileNumber],'                          ');
       Assign(Infile,inputfile[FileNumber]+'.INP');
       Reset(Infile);
       Assign(Outfile,inputfile[FileNumber]+'.OUT');
       Rewrite(Outfile);
       Writeln(Outfile,' FFSN      Fcorr1    Fcorr2    Fcorr4    Fcorr8');
       Writeln(Outfile);
       Readln(Infile);
       Teller := 0;
{        Begin benadering correctie
}
       While not Eof(Infile) Do
       Begin
          Teller := Teller + 1;
          Readln(Infile,FFSN);
          Write(Outfile,FFSN:8:4);
          Writeln(Teller:3,'    FFSN: ',FFSN:4:2);
          For Parameter := 0 TO 3 Do
          Begin
             DeltaT  := Round(Macht(2,Parameter))*0.04;
             DeltaTau:= DeltaT/Tr;
             P       := FFSN*DeltaT/D;
             G       := FFSN*Tg/D;
             R       := FFSN*Tr/D;
             Fc      := Fcorr(DeltaTau,P,G,R);
             Write(Outfile,Fc:10:5);
             Writeln(Fc:8:3);
          End;
          Writeln(Outfile);
          GotoXY(1,WhereY-5);
       End;
       Close(Outfile);
       Close(Infile);
    End;
end.
```

```
{
        Programma om de Iresp te berekenen

        Date      : 03-07-91
        Programmer: Rik van der Ploeg
}
Program IrespBer;

Uses
   Crt,Dos;

Const
   Tr         = 0.0531;
   Punten     = 10;
   MisVal     = -9999;
   Resolutie = 500;

Var
   Parameter, B, N, Delta, I, Teller          :Integer;
   DeltaT,Tau,DeltaTau,HFac                   :Real;
   IResp                                      :Array[0..20,0..3] of Real;
   Outfile1,Outfile2                          :Text;

Function Macht(Arg,Eksponent :Real) : Real;

Begin
    If Arg <> 0 Then Macht := Exp(Eksponent*Ln(Arg))
    Else  Macht := 0;
End; {Macht}

Function H( Tau :Real ) : Real;

Begin
  If (Tau >=0) and (Tau <1)  Then
        H:= HFac  {  HFac*(1-Exp(-10*Tau))  }
  Else If (Tau>=1) And (Tau<3) Then H := 0 {HFac*Exp(-10*(Tau-1))}
  Else H :=0 ;
End;  { H }

Function IntHSimp (Stappen :Integer) :Real;

Var
    Punt               : Integer;
    S, Y1, Y2, Y3,Sim  : Real;

Begin
    S   := B*0.5/Stappen;        { Stapgrootte }
    Sim := 0;
    For Punt := 1 To Stappen Do
    Begin
       Y1 :=(2*Punt-2)*S;
       Y2 :=Y1+S;
       Y3 :=Y2+S;
       Sim := Sim + H(Y1)+4*H(Y2)+H(Y3);
    End;
    IntHSimp := S*Sim/3;
End; {IntHSimp}

Function OppervlakH :Real;
```

```
Var N                    : Integer;
    Int1,Int2,Fout       : Real;

Begin
     N         := 1000;
  Int1         := IntHSimp(N);
  Int2         := IntHSimp(2*N);
  Fout         := (Int2-Int1)/15;
  OppervlakH   := Int2+Fout;
  Writeln(Int2+Fout:1:8);
End; {OppervlakH}


Function Irespint(Tau,DTau: Real;I: Integer) :Real;

Begin
  Irespint := H(Tau)*(2*H(Tau-I)-H(Tau+DTau-I)-H(Tau-DTau-I));
End;

Function IrespS (DTau : Real;I,Stappen :Integer) :Real;

Var
    Punt                 : Integer;
    S, Y1, Y2, Y3,Sim    : Real;

Begin
    S   := B*0.5/Stappen;          { Stapgrootte }
    Sim := 0;
    For Punt := 1 To Stappen Do
    Begin
       Y1 :=(2*Punt-2)*S;
       Y2 :=Y1+S;
       Y3 :=Y2+S;
       Sim := Sim + Irespint(Y1,DTau,I)+4*Irespint(Y2,DTau,I)+
                                                 Irespint(Y3,DTau,I);
    End;
    IrespS := S*Sim/3;
End; {IrespS}

Procedure BerIResp (ILimit,N :Integer);

Var Parameter, I        : Integer;
    DTau, Int1,Int2,Fout,Int : Real;

Begin
  For Parameter := 0 To 3 Do
  Begin
    Write('Cww',Round(Macht(2,Parameter)),'  :        ');
    DTau := 0.04/Tr*Macht(2,Parameter);
    For I := 0 To ILimit Do
    Begin
      GotoXY(10,WhereY);
      Write(I);
      Int1 := IrespS(DTau,I,N);
      Int2 := IrespS(DTau,I,2*N);
      Fout := (Int2-Int1)/15;
      Int  := Int2+Fout;
      Iresp [I,Parameter] := Int;
    End;
    Iresp[ILimit+1,Parameter] := MisVal;
```

```
    GotoXY(1,WhereY);
  End;
  Writeln('                                    ');
End; {BerIResp}

Begin
    {   Open output, vraag gegevens
    }
    Assign(Outfile1,'Hresp.DTS');
    Assign(Outfile2,'IRESP.OUT');
    Rewrite(Outfile1);
    Rewrite(Outfile2);
    ClrScr;
    Tau  := 0;
    HFac := 1;
    Repeat
      Tau := Tau+0.05;
    Until H(Tau)<0.001;
    B        := Round(Tau-0.05+0.5);
    Write('Berekening Oppervlakte H met HFac=1 :');
    HFac     := 1/OppervlakH;
    Writeln(Outfile1,'Tau       H(Tau)   ');
    For Teller := 0 To Resolutie Do
    Begin
      Tau := Teller/Resolutie*B;
      Writeln(Outfile1,Tau:1:3,H(Tau):9:4);
    End;
    Close(Outfile1);
    Writeln;
    Write('Aantal Stappen voor berekening van Iresp: ?');
    GotoXY(WhereX-1,WhereY);
    Readln(N);
    BerIResp(Punten+B,N);
    Writeln(Outfile2,'B: ');
    Writeln(Outfile2,B);
    Writeln(Outfile2,'      Iresp1     Iresp2     Iresp4     Iresp8');
    For I:= 0 To Punten+B Do
    Begin
      For Parameter := 0 To 3 Do
      Begin
        Write(Outfile2,Iresp[I,Parameter]:12:5);
      End;
      Writeln(Outfile2);
    End;
    Close(Outfile2);
end.
```

```
{
        Programma om de Iline te benaderen

        Date      : 29-05-91
        Programmer: Rik van der Ploeg
}
PROGRAM Iintber;

USES
   Crt;

CONST
   D    = 0.20;
   u2_3 =-0.05;
   Ex   = 2/3-u2_3;

VAR
   J, N ,Aantal                                :INTEGER;
   X,Int1,Int2,Int,
   XEinde,StapGrootte,Fout                     :REAL;
   Outfile                                     :TEXT;
Function Macht(Arg,Eksponent :Real) : Real;

Begin
    If Arg <> 0 Then Macht := Exp(Eksponent*Ln(Arg))
    Else  Macht := 0;
End; {Macht}

Function I(Y,X :Real) : Real;

Begin
     I  := (X*X+0.75*Y*Y)*Macht(X*X+Y*Y,0.5*Ex-1)*(1-Y);
End;  { I }

Function IlineS (N : Integer; X :Real) : Real;

Var
    J                  : Integer;
    H, Y1, Y2, Y3,Sim  : Real;
Begin
    H   := 0.5/N;        { Stapgrootte }
    Sim := 0;
    For J := 1 To N Do
    Begin
      Y1 :=(2*J-2)*H;
      Y2 :=Y1+H;
      Y3 :=Y2+H;
      Sim := Sim + I(Y1,X)+4*I(Y2,X)+I(Y3,X);
    End;
    IlineS := H*Sim/3;
End; {IlineS}

BEGIN
    ASSIGN(Outfile,'ILINEBER.OUT');
    REWRITE(Outfile);
    WRITELN;
    Write('XEinde :');
    Readln(XEinde);
    Write('StapGrootte :');
    Readln(StapGrootte);
```

```
    Aantal := Round(XEinde/StapGrootte);
    N      := 100;
    Writeln(Outfile,'    X          Iline');
    Writeln(Outfile);
    For J := 0 To Aantal Do
    BEGIN
       X := J*StapGrootte;
       Write(Outfile,X:10:6);
       Write(J,'    X: ',X:6:4);
       Int1    := IlineS(N,X);   {  Benader de integraal met simpson}
       Int2    := IlineS(2*N,X);
       Fout    := (Int2-Int1)/15;
       Int     := Int2+Fout;
       Writeln(Outfile,Int:13:7);
       Writeln('   Iline: ',Int:8:5,'  Fout:',Fout:10:6);
    END;
    Close(Outfile);
END.
```

B2 Programs for Crau

```
{
         Programma om U* te corrigeren
         voor opstroom en aanstroomhoek, verder
         U te berekenen  voor Crau
         Date      : 25-6-91
         Programmer: Rik van der Ploeg
}
Program CrauCor;

Uses
   Crt,Dos;

Const Ex     = 2/3;
      MisVal = -9999;

Type Datafile = File of Single;


Var  InFile,OutFile                    : Datafile;
     InVal                             : Array [0..199] Of Single;
     U,FFSN,DDSN,Rotr,UU,VV,Phi,
     UsterCor,Uster                    : Real;
     I                                 : Integer;
     Missing                           : Boolean;
     CrauFile                          : SearchRec;
     OutFileName                       : String[12];

Function Macht(Arg,Eksponent :Real) : Real;

Begin
    If Arg <> 0 Then Macht := Exp(Eksponent*Ln(Arg))
    Else  Macht := 0;
End; {Macht}

Begin
  FindFirst('CR??????.B30', Archive, CrauFile);
  While DosError = 0 Do
  Begin
    Missing := False;
    Assign(InFile,CrauFile.Name);
    Assign(OutFile,Copy(CrauFile.Name,1,8)+'.c30');
    Rewrite(OutFile);
    Reset(InFile);
    Writeln(CrauFile.Name);
    While not Eof(Infile) Do
    Begin
       For I := 0 To 199 Do
       Begin
         Read(Infile,InVal[I]);
       End;
       FFSN      := InVal[6];
       VV        := InVal[90];
       DDSN      := InVal[7];
       Rotr      := InVal[35];
       UU        := InVal[84];
       Uster     := InVal[8];
       If (DDSN=MisVal) Or (Rotr=MisVal) Then Missing := True;
       If Not(Missing) Then
       Begin
         Phi := DDSN-Rotr;
```

```
        If Phi <0 Then Phi := Phi+360;
        If Phi >180 Then Phi := Phi-360;
        If Abs(Phi) >60 Then Phi:= MisVal
        Else Phi := Phi/180*Pi;
      End Else Phi := MisVal;
      Missing := False;
      If (FFSN=MisVal) Or (VV=MisVal) Or (Phi=MisVal) Then Missing:= True;
      If Not(Missing) Then
      Begin
        U := FFSN+0.5*VV/FFSN;          {Berekening en correctie U}
        U := U/(1-0.08*Sqr(Phi));
      End Else U := MisVal;
      Missing := False;
      If (Uster=Misval) Or (UU=Misval) Or (Phi=MisVal) Then Missing:= True;
      If Not(Missing) Then
      Begin
        UsterCor := Sqrt(Sqr(Uster)+0.024*UU);       {Correctie Uster }
        UsterCor := UsterCor/Sqrt(1-0.08*Sqr(Phi));
      End Else UsterCor := MisVal;
      Missing := False;
      InVal[4] := U;
      InVal[57]:= UsterCor;
      For I := 0 To 199 Do
      Begin
        Write(Outfile,InVal[I]);
      End;
  End;
  Close(InFile);
  Close(OutFile);
  FindNext(CrauFile);
End;
```

```
{
         Programma om LOED te corrigeren
         voor opstroom en aanstroomhoek (corrected = LOBH)
         Date      : 25-6-91
         Programmer: Rik van der Ploeg
}
Program LobhCor;

Uses
   Crt,Dos;

Const Ex     = 2/3;
      Kappa  = 0.4;
      G      = 9.81;
      MisVal = -9999;

Type Datafile = File of Single;


Var  InFile,OutFile                    : Datafile;
     InVal                             : Array [0..199] Of Single;
     LOED,UsterCor,L,Uster             : Real;
     I                                 : Integer;
     Missing                           : Boolean;
     CrauFile                          : SearchRec;
     OutFileName                       : String[12];

Function Macht(Arg,Eksponent :Real) : Real;

Begin
    If Arg <> 0 Then Macht := Exp(Eksponent*Ln(Arg))
    Else  Macht := 0;
End; {Macht}

Begin
  FindFirst('CR??????.C30', Archive, CrauFile);
  While DosError = 0 Do
  Begin
    Missing := False;
    Assign(InFile,CrauFile.Name);
    Assign(OutFile,CrauFile.Name);
    Reset(OutFile);
    Reset(InFile);
    Writeln(CrauFile.Name);
    While not Eof(Infile) Do
    Begin
       For I := 0 To 199 Do
       Begin
         Read(Infile,InVal[I]);
       End;
       Missing   := False;
       LOED      := InVal[17];
       Uster     := InVal[8];
       UsterCor  := InVal[57];
       If (UsterCor=MisVal) Or (Uster=MisVal) Or (LOED=MisVal) Then
          Missing := True;
       If Not(Missing) Then
       Begin
         L        := LOED*Macht(Ustercor/Uster,3);
       End Else L := MisVal;
```

```
      Missing  := False;
      InVal[58]:= L;
      For I := 0 To 199 Do
      Begin
        Write(Outfile,InVal[I]);
      End;
  End;
  Close(InFile);
  Close(OutFile);
  FindNext(CrauFile);
End;
```

B3 Programs for Speuld

```
{
         Programma om U te berekenen en te corrigeren
         voor aanstroomhoek, voor SPEULD
         Date       : 2-7-91
         Programmer: Rik van der Ploeg
}
Program USpeuld;

Uses
   Crt,Dos;

Const MisVal = -9999;

Type Datafile = File of Single;


Var  InFile,OutFile                    : Datafile;
     InVal                             : Array [0..199] Of Single;
     U,FFSN,DDSN,Rotr,VV,Phi           : Real;
     I                                 : Integer;
     Missing                           : Boolean;
     SpeuldFile                        : SearchRec;
     OutFileName                       : String[12];

Begin
  FindFirst('SP??????.B30', Archive, SpeuldFile);
  While DosError = 0 Do
  Begin
    Missing := False;
    Assign(InFile,SpeuldFile.Name);
    Assign(OutFile,Copy(SpeuldFile.Name,1,8)+'.C30');
    Rewrite(OutFile);
    Reset(InFile);
    Writeln(SpeuldFile.Name);
    While not Eof(Infile) Do
    Begin
       For I := 0 To 199 Do
       Begin
         Read(Infile,InVal[I]);
       End;
       FFSN      := InVal[6];
       VV        := InVal[108];
       DDSN      := InVal[7];
       Rotr      := InVal[34];
       If (DDSN=MisVal) Or (Rotr=MisVal) Then Missing := True;
       If Not(Missing) Then
       Begin
         Phi := DDSN-Rotr;
         If Phi <0 Then Phi := Phi+360;
         If Phi >180 Then Phi := Phi-360;
         If Abs(Phi) >60 Then Phi:= MisVal
         Else Phi := Phi/180*Pi;
       End Else Phi := MisVal;
       Missing := False;
       If (FFSN=MisVal) Or (VV=MisVal) Or (Phi=MisVal) Then Missing:= True;
       If Not(Missing) Then
       Begin
         U := FFSN+0.5*VV/FFSN;          {Berekening en correctie U}
         U := U/(1-0.08*Sqr(Phi));
       End Else U := MisVal;
```

```
        Missing := False;
        InVal[164] := U;
        For I := 0 To 199 Do
        Begin
          Write(Outfile,InVal[I]);
        End;
    End;
    Close(InFile);
    Close(OutFile);
    FindNext(SpeuldFile);
  End;
End.
```

B4 Programs for Cabauw

```
{
        Programma om foute Cabauw gegevens om te werken en ontbrekende
        te berekenen
        voor      : Uson,Vson,DDSN,FFSN,U,U*,<UW>,<UT>,<US>,<VW>,<VT>,<VS>
        Date      : 24-6-91
        Programmer: Rik van der Ploeg
}
Program Cabcor;

Uses
   Crt,Dos;

Const Ex     = 2/3;
      MisVal = -9999;

Type Datafile = File of Single;


Var  InFile,OutFile                    : Datafile;
     InVal                             : Array [0..79] Of Single;
     DDRad,UUacc,UWacc,VVacc,FFSN,
     U,Uoud,UU,VV,UV,UW,VW,UT,US,VT,VS,
     USon,VSon,DeltaT                  : Real;
     I,Par                             : Integer;
     Missing                           : Boolean;
     CabauwFile                        : SearchRec;
     OutFileName                       : String[12];

Function Macht(Arg,Eksponent :Real) : Real;

Begin
    If Arg <> 0 Then Macht := Exp(Eksponent*Ln(Arg))
    Else  Macht := 0;
End; {Macht}

Function DDSN(U,V: Real) :Single;

Var Hoek : Single;

Begin
  If (U=MisVal) Or (V=MisVal) Then DDSN:= MisVal
  Else
  Begin
    If V = 0 Then V:= 0.000001;
    Hoek := Round(ArcTan(U/V)*180/Pi*100)/100;
    If V < 0 Then DDSN := Hoek+180
    Else If U < 0 Then DDSN := Hoek+360
    Else DDSN := Hoek;
  End;
End;

Begin
  FindFirst('CA??????.C30', Archive, CabauwFile);
  While DosError = 0 Do
  Begin
    Missing := False;
    Assign(InFile,CabauwFile.Name);
    Assign(OutFile,CabauwFile.Name);
    Reset(OutFile);
    Reset(InFile);
```

```
Writeln(CabauwFile.Name);
While not Eof(Infile) Do
Begin
   For I := 0 To 79 Do
   Begin
     Read(Infile,InVal[I]);
   End;
   USon       := -InVal[5];    {Correctie Van Verkeerde waarden in de}
   VSon       := -InVal[6];    { dataset van Cabauw }
   UU         := InVal[10];
   VV         := InVal[11];
   UV         := InVal[15];
   UW         := -InVal[16];
   UT         := -InVal[17];
   US         := -InVal[18];
   VW         := -InVal[19];
   VT         := -InVal[20];
   VS         := -InVal[21];
   InVal[5]   := USon;         {Terugzetten van de gecorrigeerde waardes}
   InVal[6]   := VSon;         {In de dataset   }
   InVal[16] := UW;
   InVal[17] := UT;
   InVal[18] := US;
   InVal[19] := VW;
   InVal[20] := VT;
   InVal[21] := VS;
   InVal[64] := DDSN(USon,VSon);
   If InVal[64]<>MisVal Then
   Begin
     DDRad     := InVal[64]/180*Pi;
     FFSN      := Sqrt(Sqr(Uson)+Sqr(Vson));
   End
   Else Begin
     DDRad := MisVal;
     FFSN  := MisVal;
   End;
   InVal[4] := FFSN;
   If (UU=MisVal) Or (UV=MisVal) Or (VV=MisVal) Or (USon=MisVal)
      Or (VSon=MisVal) Then Missing := True;
   If Not(Missing) Then        {Correctie U, berekend }
   Begin                       {met een verkeerde DDRad}
     VVacc     := UU*Sqr(Cos(DDRad))-UV*2*Sin(DDRad)*Cos(DDRad)
                                          +VV*Sqr(Sin(DDRad));
     U         := FFSN+0.5*VVacc/FFSN;
     InVal[65] := U;
     If (UW=MisVal) Or (VW=MisVal) Then Missing := True;
     If Not(Missing) Then
     Begin                  {Berekening U* }
       UUacc     := UU*Sqr(Sin(DDRad))+UV*2*Sin(DDRad)*Cos(DDRad)
                                          +VV*Sqr(Cos(DDRad));
       UWacc     := UW*Sin(DDRad)+VW*Cos(DDRad);
       If (UWacc-0.02*UUacc)<0 Then InVal[57] :=Sqrt(-(UWacc-0.02*UUacc))
       Else InVal[57] := MisVal;
     End
     Else InVal[57] := MisVal;
   End
   Else InVal[65] := MisVal;
   For I := 0 To 79 Do
   Begin
     Write(Outfile,InVal[I]);
```

```
        End;
        Missing := False;
      End;
      Close(InFile);
      Close(OutFile);
      FindNext(CabauwFile);
    End;
End.
```

```
{
        Programma om de Cww's te berekenen uit de wortel van de Dww's
        voor Cabauw
        Date       : 24-6-91
        Programmer: Rik van der Ploeg
}
Program CwwCabauw;

Uses
   Crt,Dos;

Const Ex     = 2/3;
      MisVal = -9999;

Type Datafile = File of Single;


Var  InFile,OutFile                          : Datafile;
     InVal                                   : Array [0..79] Of Single;
     DDRad,VVacc,FF,U,USon,VSon,UU,VV,
     UV,DeltaT                               : Real;
     I,Par                                   : Integer;
     Missing                                 : Boolean;
     CabauwFile                              : SearchRec;
     OutFileName                             : String[12];

Function Macht(Arg,Eksponent :Real) : Real;

Begin
    If Arg <> 0 Then Macht := Exp(Eksponent*Ln(Arg))
    Else  Macht := 0;
End; {Macht}

Function DDSN(U,V: Real) :Single;

Var Hoek : Single;

Begin
  If (U=MisVal) Or (V=MisVal) Then DDSN:= MisVal
  Else
  Begin
    If U = 0 Then U:= 0.000001;
    Hoek := Round(ArcTan(V/U)*180/Pi*10)/10;
    If U < 0 Then DDSN := Hoek+180
    Else If V < 0 Then DDSN := Hoek+360
    Else DDSN := Hoek;
  End;
End;

Begin
  FindFirst('CA??????.B30', Archive, CabauwFile);  {Using the original Cabauw-}
  While DosError = 0 Do                            {files  }
  Begin
    Missing := False;
    Assign(InFile,CabauwFile.Name);
    Reset(InFile);
    Writeln(CabauwFile.Name);
    OutFileName := Copy(CabauwFile.Name,1,8)+'.C30';
    Assign(OutFile,OutFileName);
    Rewrite(OutFile);
```

```
  While not Eof(Infile) Do
  Begin
     For I := 0 To 79 Do
     Begin
       Read(Infile,InVal[I]);
     End;
     USon       := -InVal[5];          {Before correction by CABCOR.PAS }
     VSon       := -InVal[6];
     UU         := InVal[10];
     VV         := InVal[11];
     UV         := InVal[15];
     If (USon=MisVal) Or (VSon=MisVal) Or (UU=MisVal) Or (VV=MisVal)
        Or (UV=MisVal) Then Missing := True;
     InVal[64] := DDSN(USon,VSon);
     If Not(Missing) Then
     Begin
       DDRad      := InVal[64]/180*Pi;
       FF         := Sqrt(Sqr(USon)+Sqr(VSon));
       VVacc      := UU*Sqr(Sin(DDRad))-UV*2*Sin(DDRad)*Cos(DDRad)
                                              +VV*Sqr(Cos(DDRad));
       U          := FF+0.5*VVacc/FF;
       For Par := 1 To 3 Do
       Begin
         DeltaT := Round(Macht(2,Par))*0.04;
         If InVal[36+Par]<> MisVal Then
            InVal[36+Par] := Sqr(InVal[36+Par])/Macht(DeltaT*U,Ex)
         Else InVal[36+Par] := MisVal;
       End;
     End;
     For I := 0 To 79 Do
     Begin
       Write(Outfile,InVal[I]);
     End;
     Missing := False;
  End;
  Close(OutFile);
  CLose(InFile);
  FindNext(CabauwFile);
End;
```

```
{
        Programma om Lobh te berekenen  voor Cabauw
        Date       : 24-6-91
        Programmer: Rik van der Ploeg
}
Program Lobh;

Uses
   Crt,Dos;

Const Ex      = 2/3;
      Kappa   = 0.4;
      G       = 9.81;
      MisVal  = -9999;

Type Datafile = File of Single;


Var  InFile,OutFile                          : Datafile;
     InVal                                   : Array [0..79] Of Single;
     U,Uster,T,WS,ThetaV,WThetaV             : Real;
     I,Par                                   : Integer;
     Missing                                 : Boolean;
     CabauwFile                              : SearchRec;
     OutFileName                             : String[12];

Function Macht(Arg,Eksponent :Real) : Real;

Begin
    If Arg <> 0 Then Macht := Exp(Eksponent*Ln(Arg))
    Else  Macht := 0;
End; {Macht}

Begin
  FindFirst('CA??????.C30', Archive, CabauwFile);
  While DosError = 0 Do
  Begin
    Missing := False;
    Assign(InFile,CabauwFile.Name);
    Assign(OutFile,CabauwFile.Name);
    Reset(OutFile);
    Reset(InFile);
    Writeln(CabauwFile.Name);
    While not Eof(Infile) Do
    Begin
       For I := 0 To 79 Do
       Begin
         Read(Infile,InVal[I]);
       End;
       U          := InVal[65];
       Uster      := InVal[57];
       T          := InVal[9];
       WS         := InVal[23];
       If (U=MisVal) Or (Uster=MisVal) Or (T=MisVal) Or (WS=MisVal)
          Then Missing := True;
       If Not(Missing) Then
       Begin
         ThetaV   := (T+273.15)+0.104;
         WThetaV  := WS-2/403*U*Sqr(Uster);
         InVal[66]:= -ThetaV*Macht(Uster,3)/WThetaV/Kappa/G;
```

```
        End
        Else InVal[66] := MisVal;
        For I := 0 To 79 Do
        Begin
          Write(Outfile,InVal[I]);
        End;
        Missing := False;
      End;
      Close(InFile);
      Close(OutFile);
      FindNext(CabauwFile);
    End;
End.
```

LITERATURE

Anselmet, F., Cagne, Y., Hopfinger, E.J. and Antonia, R.A. (1984): 'Velocity structure functions in turbulent shear flows.', J.Fluid Mech. 140, 63-89

Bosveld, F.C., J.G. van der Vliet and W.A.A. Monna (1995). The Speulderbos experiment, 1988-1989. To be published, KNMI, TR.

Bouwman, P. (1990): 'Flux-profile relationships in the nocturnal boundary layer', KNMI, TR-130

Busch, N.E. and Panofsky, H.A. (1968): 'Recent spectra of atmospheric turbulence.', Quart.J.Roy.Met.Soc. 94, 132-148

Duyzer, J.H. and Bosveld, F.C. (1988): 'Measurement of dry deposition fluxes of O_3, NO_x, SO_2 and particles ofer grass/heath land vegetation and the influence of surface inhomogeneity', TNO-Delft, MT R88/111

Frisch, U., Sulem, P.L. and Nelkin, M. (1978): 'A simple dynamical model of intermittent fully developed turbulence', J.Fluid Mech. 87, 719-736

Garratt, J.R. (1972): 'Studies of turbulence in the surface layer over water. Part II. Production and dissipation of velocity and temperature fluctuations.', Quart.J.Roy.Met.Soc. 98, 190-201

Hinze (1959): 'Turbulence', New York, Mc Graw-Hill

Kai, K. (1982): 'Statistical characterisitcs of turbulence and the budget of turbulent energy in the surface boundary layer.', Envir.Res.Center Papers, no.1 (Univ. of Tsukaba Japan)

Kaijo Denki, 'Digitized Ultrasonic anemometer thermometer model DAT-300, Instruction Manual, Kaijo Denki Co. LTD

Kaimal, J.C., Wyngaard, J.C., Izumi, Y. and Coté, O.R. (1972): 'Spectral characteristics of surface-layer turbulence', Quart.J.R.Met.Soc., 98, 563-589

Kohsiek, W. (1982): 'Measuring C_T^2, C_Q^2 and C_{TQ} in the unstable surface layer, and relations to the vertical fluxes of heat and moisture', Bound. Layer Met., 24, 89-107

Kohsiek, W., van der Vliet, J.G. and Monna, W.A.A., (1988): 'CRAU 1987: The KNMI contribution', KNMI, TR-110

Kolmogorov, A.N. (1962): 'A refinement of previous hypothesis concerning the local structure of turbulence in a viscous incompressible fluid at high Reynolds number', J.Fluid Mech. 13, 82-85

Monna, W.A.A. and Van der Vliet, J.G. (1987): 'Facilities for research and weather observations on the 213m tower at Cabauw and at remote locations, KNMI WR 87-5

Nieuwstadt, F. (1989): 'Turbulentie, dictaat bij het college turbulentie A (b60A)', TU-Delft, Faculteit der Werktuigbouwkunde, Vakgr. stromingsleer, Delft, Netherlands (in Dutch)

Oppenheim, A.V., Willsky, A.S. and Young, I.T. (1983): 'Signals and systems', Prentice/Hall International, USA

Schotanus, P. (1982): 'Turbulente fluxen in inhomogene omstandigheden', KNMI WR 82-3 (in Dutch)

Stewart, R.W. (1963): 'Reconciliation of the available experimental data concerning the spectrum and asymmetry of locally isotropic turbulence', Doklady Akad. Nauk SSSR, 152, no2, 324-326

Tennekes, H. and Lumley, J.L. (1972): 'A first course in turbulence', MIT-Press, USA

Tennekes, H. (1973): 'Intermittency of the small-scale structure of atmospheric turbulence', Bound. Layer Met., 4, 241-250

Van Atta, C.W. and Chen, W.Y. (1970): 'Structure functions of turbulence in the atmospheric boundary layer over the ocean', J.Fluid Mech. 44, 145-159

Wieringa, J. (1980): 'A revaluation of the Kansas mast influence on measurements of stress and cup anemometer overspeeding.', Bound.Layer Met. 18, 411-430

Wyngaard, J.C., Izumi, Y. and Collins Jr., S.A. (1971): 'Behavior of the refractive-index-structure parameter near the ground.', J.Opt.Soc.Am. 61, 1646-1650

Wyngaard, J.C. and Coté, O.R. (1971): 'The budgets of turbulent kinetic energy and temperature variance in the atmospheric surface layer.', J.Atmos.Sci. 28, 190-201